別紙４

研究成果の刊行に関する一覧表

雑誌

発表者氏名	論文タイトル名	発表誌名	巻号	ページ	出版年
Brumme, ZL., Li, C., Miura, T., Sela, J., Rosato, PC., Brumme, CJ., Markle, T., Martin, E., Block, BL., Trocha, T., Kadie, CM., Allen, TM., Pereyra, F., Heckerman, D., Walker, BD., Brockman, MA	Reduced replication capacity of NL4-3 recombinant viruses encoding RT-Integrase sequences from HIV-1 elite controllers.	*Journal of Acquired Immune Deficiency Syndrome*	56	100-108	2011
Nakamura, H., Miyazaki, N., Hosoya, N., Koga, M., Odawara, T., Kikuchi, T., Koibuchi, T., Kawana-Tachikawa, A., Fujii, T., Miura, T., Iwamoto, A.	Long-term successful control of super-multidrug-resistant human immunodeficiency virus type 1 infection by a novel combination therapy of raltegravir, etravirine, and boosted-darunavir.	J Infect Chemother	17	105-110	2011
Gesprasert G, Wichukchinda N, Mori M, Shiino T, Auwanit W, Sriwanthana B, Pathipvanich P, Sawanpanyalert P, Miura T, Auewarakul P, Thitithanyanont A, Ariyoshi K	HLA-associated immune pressure on Gag protein in CRF01_AE-infected individuals and its association with plasma viral load	PLoS One	5	e11179	2010
Miura, T., Z. L. Brumme, M. A. Brockman, P. Rosato, J. Sela, C. J. Brumme, F. Pereyra, D. E. Kaufmann, A. Trocha, B. L. Block, E. S. Daar, E. Connick, H. Jessen, A. D. Kelleher, E. Rosenberg, M. Markowitz, K. Schafer, F. Vaida, A. Iwamoto, S. Little, and B. D. Walker.	Impaired replication capacity of acute/early viruses in persons who become HIV controllers	J Virol	84	7581-7591	2010
Wright, JK., Brumme, ZL., Carlson, JM., Heckerman, D., Kadie, CM., Brumme, CJ., Wang, B., Losina, E., Miura, T., Chonco, F., van der Stok, M., Mncube, Z., Bishop, K., Goulder, PJ., Walker, BD., Brockman, MA.,	Gag-protease-mediated replication capacity in HIV-1 subtype C chronic infection: associations with HLA type and clinical parameters.	J Virol	84	10820-10831	2010
Julg, B., Pereyra, F., Buzon, MJ., Piechocka-Trocha, A., Clark, MJ., Baker, BM., Lian, J., Miura, T., Martinez-Picado, J., Addo, MM., Walker, BD	Infrequent recovery of HIV from but robust exogenous infection of activated CD4(+) T cells in HIV elite controllers.	Clin Infect Dis	51	233-238	2010

Brockman, M. A., Brumme, ZL., Brumme, CJ., Miura, T., Sela, J., Rosato, PC., Kadie, CM., Carlson, JM., Markle, TJ., Streeck, H., Kelleher, AD., Markowitz, M., Jessen, H., Rosenberg, E., Altfeld, M., Harrigan, PR., Heckerman, D., Walker, BD., Allen, TM.	Early selection in Gag by protective HLA alleles contributes to reduced HIV-1 replication capacity that may be largely compensated in chronic infection	J Virol.	84	11937-11949	2010

J Infect Chemother (2011) 17:105–110
DOI 10.1007/s10156-010-0082-4

CASE REPORT

Long-term successful control of super-multidrug-resistant human immunodeficiency virus type 1 infection by a novel combination therapy of raltegravir, etravirine, and boosted-darunavir

Hitomi Nakamura · Naoko Miyazaki · Noriaki Hosoya · Michiko Koga · Takashi Odawara · Tadashi Kikuchi · Tomohiko Koibuchi · Ai Kawana-Tachikawa · Takeshi Fujii · Toshiyuki Miura · Aikichi Iwamoto

Received: 9 April 2010 / Accepted: 28 May 2010 / Published online: 30 June 2010

Abstract Drug-resistant virus infection has been a major hurdle in the management of human immunodeficiency virus type 1 (HIV-1) infection. Recently, three novel antiretrovirals [raltegravir (RAL), etravirine (ETR), and darunavir (DRV)] were introduced into the market almost simultaneously, and salvage regimens containing these three antiretrovirals have been reported to exhibit strong potency against drug-resistant HIV-1 infection. However, the sustainability of such regimens remains unclear, particularly for patients infected with multidrug-resistant viruses. Here we report a case of super-multidrug-resistant HIV-1 infection which has been successfully controlled by novel combination therapy including RAL, ETR, and DRV for over 2 years, indicating that the novel combination could become an ultimate weapon against drug-resistant HIV infection and could alter the landscape of HIV salvage therapy.

Keywords Salvage therapy · Antiretrovirals · Drug resistance · Darunavir · Raltegravir · Etravirine · Human immunodeficiency virus type 1

H. Nakamura · N. Hosoya · M. Koga · T. Odawara · T. Kikuchi · A. Kawana-Tachikawa · T. Miura (✉) · A. Iwamoto
Division of Infectious Disease, Advanced Clinical Research Center, The Institute of Medical Science, The University of Tokyo, 4-6-1 Shirokanedai, Minato-ku, Tokyo 108-8639, Japan
e-mail: miura523@ims.u-tokyo.ac.jp

N. Miyazaki
Japan Foundation for AIDS Prevention, Tokyo, Japan

N. Miyazaki · T. Koibuchi · T. Fujii · A. Iwamoto
Department of Infectious Diseases and Applied Immunology, The Institute of Medical Science, The University of Tokyo, Tokyo, Japan

Introduction

Human immunodeficiency virus type 1 (HIV-1) was discovered 27 years ago, but the development of HIV vaccines has been unsuccessful. Fortunately, a handful of antiretrovirals have been developed and are widely available, at least in resource-rich settings. Although the eradication of viruses from infected human bodies cannot be achieved at the present time, the emergence of triple combination therapies of antiretrovirals in the late 1990s altered the whole picture of HIV management completely: antiretroviral therapies (ARTs) consisting of 2 nucleoside analogue reverse transcriptase inhibitors (NRTIs) and either one protease inhibitor (PI) or one non-nucleoside analogue reverse transcriptase inhibitor (NNRTI) have enabled viremia suppression to the limit of detection by commercial HIV quantification assay (<30–50 RNA copies/ml plasma). However, viral drug-resistance mutations often evolve under incomplete viremia control [1–3]. Many HIV-infected individuals who had been exposed to single or dual NRTIs before the introduction of triple combination therapy have experienced virologic failure due to the emergence of NRTI-resistant mutants, which, in turn, has facilitated the evolution of mutations resistant to PIs and/or NNRTIs. As a consequence, individuals who acquired viruses in the early days of the HIV epidemic have been suffering from a high level of antiretroviral-resistant HIV infection and progressive disease. Salvage therapies for such patients guided by viral genotypic resistance testing are usually difficult and unsuccessful.

In 2007, three new antiretrovirals were introduced into the market: raltegravir (RAL), an integrase inhibitor that belongs to a novel class of antiretrovirals, inhibiting the viral enzyme integrase [4, 5]; and etravirine (ETR) and

darunavir (DRV), a novel NNRTI and a novel PI, respectively, both of which were reported to have little cross-resistance to other antiretrovirals [6–11]. We here report a case of super-multidrug-resistant HIV-1 infection in which viremia was successfully controlled by a novel salvage regimen composed of lamivudine, RAL, ETR, and boosted-DRV. Remarkably, the new regimen demonstrated not only strong antiviral potency but also excellent sustainability, even in the presence of viral mutations associated with resistance to ETR and DRV, indicating that regimens including RAL/ETR/boosted-DRV could alter the landscape of salvage therapy for multidrug resistant HIV-1 infection.

Case report

A Japanese man who has sex with men was documented to be infected with HIV-1 in 1996 when he was 29 years old; his CD4+ T-cell count was 81/μl at the time of diagnosis. Shortly after that, he participated in a clinical trial of ART, receiving dual combination treatment composed of zidovudine (AZT) and indinavir (IDV), which raised his CD4+ T cell count from 40/μl to over 300/μl temporarily, but his plasma virus load (pVL) had been only partially controlled and stayed at over 50,000 RNA copies/ml (Fig. 1), despite his good adherence to the medication. A year later, the treatment was switched to a triple combination therapy composed of stavudine/lamivudine/nelfinavir (d4T/3TC/NFV), but this failed to suppress viremia as well. The first drug-resistance genotyping test was performed in 1997, revealing multidrug-resistant mutations in his autologous plasma viral sequence, including those for both NRTIs and PIs (Fig. 1). His treatment regimen had been changed a number of times thereafter; yet none of the regimens could sustain viremia control. Eventually his CD4+ T-cell count fell below 50/μl by the end of 2005. Before the novel combination therapy including RAL/ETR/DRV was implemented in November 2007, he had experienced total of 15 different antiretrovirals, including 6 NRTIs, 7 PIs, a single NNRTI, and a fusion inhibitor (including emtricitabine and fosamprenavir, which are functionally identical to lamivudine and amprenavir, respectively; and excluding ritonavir, which was used for booster purposes). As shown in Fig. 1 and Table 1, an enormous numbers of mutations associated with antiretroviral resistance, including those associated with a fusion inhibitor (enfuvirtide) had accumulated in his plasma autologous viral sequences (Genbank accession No. GU951450-456), indicating that no effective salvage regimens had been left for him according to the availability of antiretrovirals before 2007.

Three antiretrovirals, RAL, ETR, and DRV, were introduced into the market almost simultaneously in 2007. RAL is an integrase inhibitor which has a mechanism of action completely different from that of any other antiretrovirals; and ETR and DRV are a novel NNRTI and a novel PI, respectively, both of which were reported to have little cross-resistance to older drugs. A novel combination therapy composed of 3TC/RAL/ETR/boosted-DRV was initiated for this patient on November 1st 2007. RAL and ETR had been imported from abroad because they were not approved in Japan at the time of the initiation of the salvage therapy. No major adverse events were observed, but mild skin eruption developed shortly after the starting of the new regimen, which was probably attributable to ETR administration [7]. The new regimen exhibited strong potency, reducing pVL from 130,000 to 500 RNA copies/ml over 25 days, and raising his CD4+ T-cell count from 42 to 276 cells/μl over 10 months (Fig. 1). Of importance, the viremia has been suppressed for over 96 weeks (2 years), a period that is often considered as a benchmark of the sustainability of effective antiretroviral regimens.

Although his pVL was well controlled, it had been detectable (fluctuating at around 100–300 RNA copies/ml, measured by the Roche TaqMan® (Roche, Basel, Switzerland) HIV-1 test, which replaced the previous Roche Amplicore® (Roche, Basel, Switzerland) HIV-1 monitor test ver1.5 in early 2008 in Japan). However, as is widely known, it was revealed that the Roche TaqMan® assay was inaccurate at the low end of the dynamic range [12, 13]; moreover, there was a problem with the blood collection tube used for HIV-RNA quantification in Japan, and this was also considered to have contributed to incorrect values for HIV-RNA (reported on the Roche website: http://www.roche-diagnostics.jp/pdf/product/md/taqman_hiv.pdf). Therefore, we repeated HIV-RNA quantification, using the Abbott Real-time HIV-1 test (Abbott, Abbott Park, IL, USA) that had been demonstrated to have an excellent correlation to the Roche Amplicore® HIV-1 monitor test ver1.5 [14, 15]. And we found that the pVL was only 62 RNA copies/ml for the plasma that had been determined as 300 RNA copies/ml by the Roche TaqMan® HIV-1 test; furthermore, after all of the issues related to the Roche TaqMan® HIV-1 test were completely solved, the first HIV-RNA quantification by the Roche TaqMan® assay, performed in February 2010, was less than 40 RNA copies/ml (Fig. 1), these tests collectively indicating that the viremia has been successfully controlled to below or around the detection limit for more than 2 years.

Viral drug-resistance genotyping was performed on a total of 27 occasions since the first ART had been initiated for the present patient in 1997 (Fig. 1). In his autologous plasma viral sequences, a number of resistance-associated mutations for all of the conventional classes of antiretrovirals (NRTIs, NNRTIs, and PIs) had been accumulated [according to the HIV-1 genotypic resistance interpretation algorithm provided by Stanford

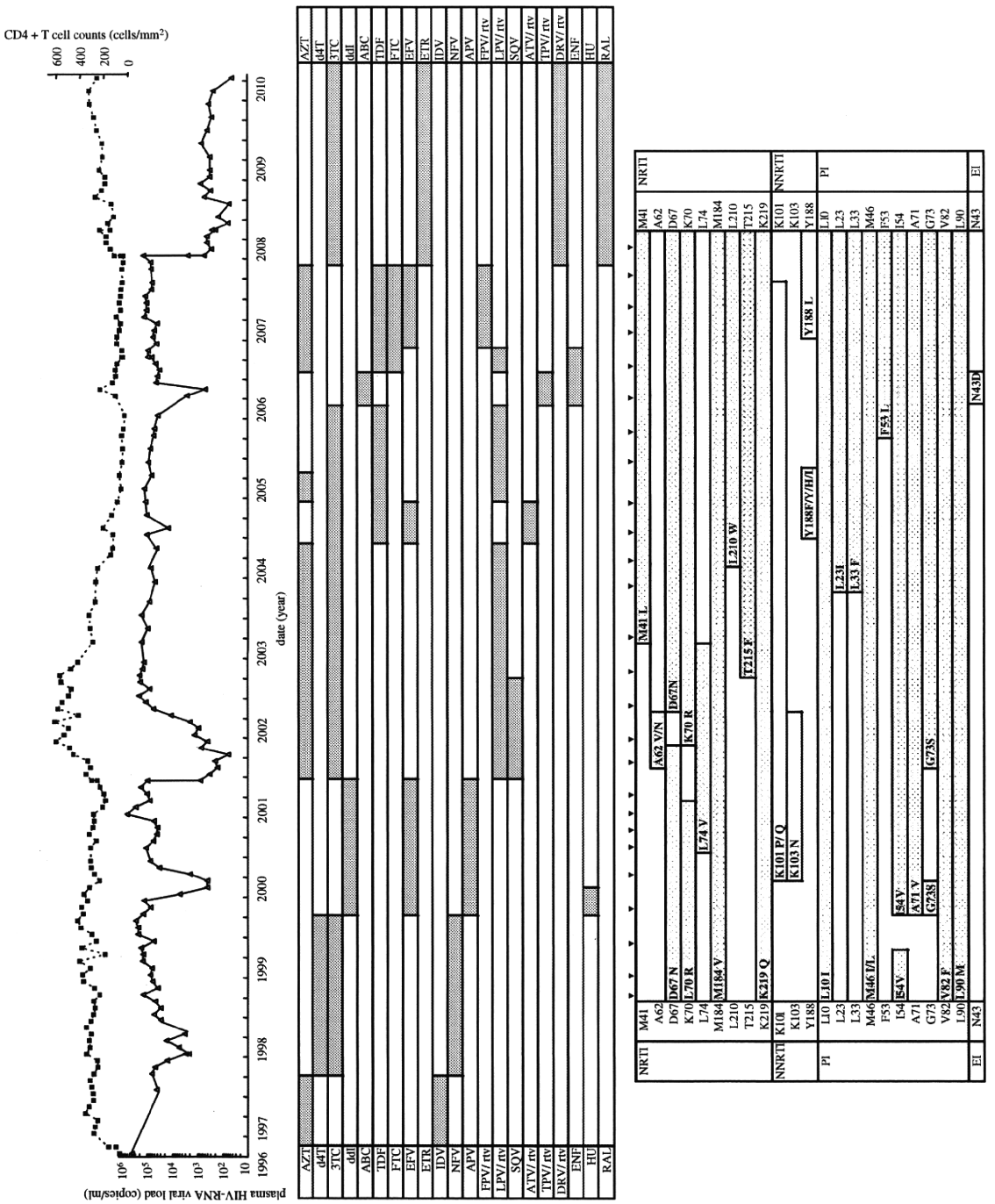

Fig. 1 Clinical course of a Japanese man infected with super-multidrug-resistant human immunodeficiency virus type 1 (the presented case). In the *upper panel*, *solid* and *dashed lines* indicate HIV-RNA level and CD4+ T cell count in the peripheral blood. The *middle panel* shows periods during which each of the antiretrovirals was prescribed; the names of the antiretrovirals follow standard abbreviations (see Table 1), except for *HU* and *ENF*, which indicate hydroxyurea and enfuvirtide, respectively. *Inverted solid triangles* between the middle and lower panels indicate sampling points for drug-resistance genotyping. The *lower panel* displays the major viral resistance mutations detected according to the HIV Drug Resistance Database of Stanford University. *APV* amprenavir, *RAL* raltegravir, *rtv* ritonavir

Table 1 Viral drug resistance interpretation

Class	Drugs	Sensitivity
NRTI[a]	Zidovudine (AZT)	High-level resistance
	Lamivudine (3TC)	High-level resistance
	Stavudine (d4T)	High-level resistance
	Didanosine (ddI)	Intermediate resistance
	Abacavir (ABC)	High-level resistance
	Tenofovir (TDF)	Intermediate resistance
	Emtricitabine (FTC)	High-level resistance
NNRTI[a]	Delavirdine (DLV)	High-level resistance
	Efavirenz (EFV)	High-level resistance
	Etravirine (ETR)	Intermediate resistance
	Nevirapine (NVP)	High-level resistance
PI[a,b]	Atazanavir/r (ATV/r)	High-level resistance
	Darunavir/r (DRV/r)	Low-level resistance
	Fosamprenavir/r (FPV/r)	High-level resistance
	Indinavir/r (IDV/r)	High-level resistance
	Lopinavir/r (LPV/r)	High-level resistance
	Nelfinavir/r (NFV/r)	High-level resistance
	Saquinavir/r (SQV/r)	High-level resistance
	Tipranavir/r (TPV/r)	Intermediate resistance
Fusion inhibitor[c]	Enfuvirtide (ENF)	10–20 fold reduced susceptibility
CCR5 inhibitor[d]	Maraviroc	Potentially harboring X4 virus

Based upon the autologous viral sequence obtained from November 2007

NRTI nucleoside analogue reverse transcriptase inhibitor, *NNRTI* non-nucleoside analogue reverse transcriptase inhibitor, *PI* protease inhibitor

[a] According to HIV-1 genotypic resistance interpretation algorithm provided by Stanford University (http://hivdb.stanford.edu/pages/algs/HIVdb.html)

[b] Small letter 'r' indicates ritonavir for booster purposes

[c] According to Stanford University HIV Drug Resistance Database (http://hivdb.stanford.edu/)

[d] According to the geno2pheno algorithm (http://coreceptor.bioinf.mpi-inf.mpg.de/)

University (http://hivdb.stanford.edu/pages/algs/HIVdb.html)]. The virus was also found to be resistant to a fusion inhibitor (enfuvirtide). Notably, the autologous plasma viral sequences in the presented case were carrying some resistance-mutations to both DRV and ETR at the time of initiation of the new salvage regimen (Table 1): V11I and L33F substitutions were observed that had been reported as DRV resistance mutations in the POWER/DUET study (6th European HIV Drug Resistance Workshop, 2008); likewise, a K101P substitution was found in the RT sequence known to reduce susceptibility to ETR by sixfold [16]; and finally Y188L, which confers low-level resistance to ETR, was also detected. These findings indicated that although only RAL was a fully active antiretroviral in the presented case (RAL resistance mutations are rarely seen in RAL-naïve patients), virus replication has been successfully controlled by the novel regimen for over 2 years.

Discussion

The patient in the case presented here had experienced almost all of the conventional antiretrovirals, including a fusion inhibitor, prior to the initiation of the new salvage regimen. Multidrug-resistance mutations had accumulated in his autologous plasma viral sequences, indicating that no effective regimens were left for this case before 2007; therefore, the infection could be called a "super-multidrug-resistant HIV infection". The successful viremia control for over 2 years by the novel salvage regimen including three recently approved antiretrovirals, RAL, ETR, and DRV, strongly indicated that this novel combination could become an ultimate weapon against drug-resistant HIV-1 infection.

The strong potency of a regimen containing RAL/ETR/DRV has been reported recently in the French TRIO study, which demonstrated successful viremia control in

individuals infected with multidrug-resistant viruses [17]. However, the duration of the follow-up of the study was limited to 48 weeks, and the enrolled patients seemed not to have very advanced diseases: the median CD4+ T-cell count was relatively high (255/μl), and the median pVL was relatively low (4.2 $\log_{10}$ RNA copies/ml). Furthermore, the median numbers of viral drug-resistance mutations observed in the studied subjects were limited [4 for PIs (only primary mutations were counted), 6 for NRTIs, and 1 for NNRTIs]. Therefore, the durability of the regimen containing these three newly approved antiretrovirals had remained unanswered, particularly for patients with advanced cases infected with viruses that had low to intermediate resistance to ETR and/or DRV. The patient presented here had an advanced disease, having a very low CD4+ T-cell count (<50/μl) and a high pVL (50,000–100,000 RNA copies/ml), even under AZT/tenofovir (TDF)/emtricitabine (FTC)/efavirenz (EFV)/fosamprenavir (FPV)/ritonavir (rtv) treatment (Fig. 1), and harboring viruses carrying numerous resistance mutations [7 for PIs (only primary mutations), 9 for NRTIs, and 3 for NNRTIs], though displaying no AIDS-defining illness. The over 2 years of sustained viremia control and immunological improvement observed in this patient demonstrated robust control of super-multidrug-resistant HIV infection by this novel combination therapy.

The majority of viral mutations selected for under ART pressure confer cross-resistance to other antiretrovirals, and this has been hampering HIV salvage therapy for a long time. Notably, the presented case suggested that a low to intermediate level of viral resistance to some of the components of this novel regimen may not necessarily result in treatment failure.

In the presented case, lamivudine (3TC) was added to the salvage regimen, in the expectation of maintaining the M184V RT mutation, which is known to be selected for under lamivudine pressure and to impair viral replication capacity considerably [18, 19]. However, as of now, it has not been elucidated whether NRTIs should be added to the combination of RAL/ETR/DRV. Thus, it would be warranted to investigate whether the addition of NRTIs would have beneficial effects for long-term viremia control; likewise, it would be warranted to investigate whether there are advantages in continuing with antiretrovirals to which viruses have already become resistant, aiming to maintain fitness-reducing viral mutations as a dominant form in vivo.

Another novel-class antiretroviral, maraviroc, which blocks HIV binding to the coreceptor CCR5, could have been used as a component of the salvage therapy for the present patient; however, to date, the prescription of maraviroc requires a demonstration of the nonexistence of CXCR4-tropic viruses in peripheral blood. We retrospectively examined the V3-loop sequences of the viral envelope gene at the time of initiation of the novel salvage therapy and found that one of the 5 clones obtained was a CXCR4-tropic virus according to the 'geno2pheno' algorithm (http://coreceptor.bioinf.mpi-inf.mpg.de/), which is widely accepted as a predictor of viral coreceptor usage [20, 21], thereby suggesting that maraviroc would not be a useful option for the treatment of the present patient (Genbank accession No: GU951445-449).

In conclusion, a salvage antiretroviral regimen including RAL in combination with ETR and boosted-DRV could become an ultimate weapon against multidrug-resistant HIV-1 infection and could change the landscape of HIV salvage therapy in the near future.

Acknowledgments This study was supported by a grant for 'Nation Wide Drug Resistance HIV Surveillance Study in Acutely and Chronically Infected HIV-1 Patients in Japan' of the Ministry of Health Labor and Welfare in Japan, and by 'the Clinical Study Group for AIDS Drugs' of the Japan Health Sciences Foundation. Etravirine was provided by Tibotec for compassionate use; and raltegravir was obtained through the Expanded Access Program by Merck & Co., Inc. (Darmstadt, Germany). Written informed consent was obtained from the presented patient, and the study was approved by the Institutional Review Board at the Institute of Medical Science, The University of Tokyo. The authors declare no conflicts of interests.

References

1. Bailey J, Blankson JN, Wind-Rotolo M, Siliciano RF. Mechanisms of HIV-1 escape from immune responses and antiretroviral drugs. Curr Opin Immunol. 2004;16:470–6.
2. de Mendoza C, O Gallego, Soriano V. Mechanisms of resistance to antiretroviral drugs—clinical implications. AIDS Rev. 2002;4:64–82.
3. Kuritzkes DR. HIV resistance: frequency, testing, mechanisms. Top HIV Med. 2007;15:150–4.
4. Grinsztejn B, Nguyen BY, Katlama C, Gatell JM, Lazzarin A, Vittecoq D, et al. Safety and efficacy of the HIV-1 integrase inhibitor raltegravir (MK-0518) in treatment-experienced patients with multidrug-resistant virus: a phase II randomised controlled trial. Lancet. 2007;369:1261–9.
5. Steigbigel RT, Cooper DA, Kumar PN, Eron JE, Schechter M, Markowitz M, et al. Raltegravir with optimized background therapy for resistant HIV-1 infection. N Engl J Med. 2008;359:339–54.
6. Lazzarin A, Campbell T, Clotet B, Johnson M, Katlama C, Moll A, et al. Efficacy and safety of TMC125 (etravirine) in treatment-experienced HIV-1-infected patients in DUET-2: 24-week results from a randomised, double-blind, placebo-controlled trial. Lancet. 2007;370:39–48.
7. Madruga JV, Cahn P, Grinsztejn B, Haubrich R, Lalezari J, Mills A, et al. Efficacy and safety of TMC125 (etravirine) in treatment-experienced HIV-1-infected patients in DUET-1: 24-week results from a randomised, double-blind, placebo-controlled trial. Lancet. 2007;370:29–38.
8. Molina JM, Cohen C, Katlama C, Grinsztejn B, Timerman A, Pedro Rde J, et al. Safety and efficacy of darunavir (TMC114) with low-dose ritonavir in treatment-experienced patients: 24-week results of POWER 3. J Acquir Immune Defic Syndr. 2007;46:24–31.

9. Molina JM, Hill A. Darunavir (TMC114): a new HIV-1 protease inhibitor. Expert Opin Pharmacother. 2007;8:1951–64.
10. Poveda E, de Mendoza C, Martin-Carbonero L, Corral A, Briz V, Gonzalez-Lahoz J, et al. Prevalence of darunavir resistance mutations in HIV-1-infected patients failing other protease inhibitors. J Antimicrob Chemother. 2007;60:885–8.
11. Poveda E, Garrido C, de Mendoza C, Corral A, Cobo J, Gonzalez-Lahoz J, et al. Prevalence of etravirine (TMC-125) resistance mutations in HIV-infected patients with prior experience of non-nucleoside reverse transcriptase inhibitors. J Antimicrob Chemother. 2007;60:1409–10.
12. Damond F, Roquebert B, Benard A, Collin G, Miceli M, Yeni P, et al. Human immunodeficiency virus type 1 (HIV-1) plasma load discrepancies between the Roche COBAS AMPLICOR HIV-1 MONITOR Version 1.5 and the Roche COBAS AmpliPrep/COBAS TaqMan HIV-1 assays. J Clin Microbiol. 2007;45:3436–8.
13. Yao JD, Germer JJ, Damond F, Roquebert B, Descamps D. Plasma load discrepancies between the Roche Cobas Amplicor human immunodeficiency virus type 1 (HIV-1) Monitor version 1.5 and Roche Cobas AmpliPrep/Cobas TaqMan HIV-1 assays. J Clin Microbiol. 2008;46:834. author reply 834.
14. Schutten M, Peters D, Back NK, Beld M, Beuselinck K, Foulongne V, et al. Multicenter evaluation of the new Abbott RealTime assays for quantitative detection of human immunodeficiency virus type 1 and hepatitis C virus RNA. J Clin Microbiol. 2007;45:1712–7.
15. Scott LE, Noble LD, Moloi J, Erasmus L, Venter WD, Stevens W. Evaluation of the Abbott m2000 RealTime human immunodeficiency virus type 1 (HIV-1) assay for HIV load monitoring in South Africa compared to the Roche Cobas AmpliPrep-Cobas Amplicor, Roche Cobas AmpliPrep-Cobas TaqMan HIV-1, and BioMerieux NucliSENS EasyQ HIV-1 assays. J Clin Microbiol. 2009;47:2209–17.
16. Vingerhoets J, Tambuyzer L, Azijn H, Hoogstoel A, Nijs S, Peeters M, et al. Resistance profile of etravirine: combined analysis of baseline genotypic and phenotypic data from the randomized, controlled Phase III clinical studies. AIDS. 2010;24(4):503–14.
17. Yazdanpanah Y, Fagard C, Descamps D, Taburet AM, Colin C, Roquebert B, et al. High rate of virologic suppression with raltegravir plus etravirine and darunavir/ritonavir among treatment-experienced patients infected with multidrug-resistant HIV: results of the ANRS 139 TRIO trial. Clin Infect Dis. 2009;49:1441–9.
18. Wainberg MA. The impact of the M184V substitution on drug resistance and viral fitness. Expert Rev Anti Infect Ther. 2004;2:147–51.
19. Wei X, Liang C, Gotte M, Wainberg MA. The M184V mutation in HIV-1 reverse transcriptase reduces the restoration of wild-type replication by attenuated viruses. AIDS. 2002;16:2391–8.
20. Sierra S, Kaiser R, Thielen A, Lengauer T. Genotypic coreceptor analysis. Eur J Med Res. 2007;12:453–62.
21. Saracino A, Monno L, Punzi G, Cibelli DC, Tartaglia A, Scudeller L, et al. HIV-1 biological phenotype and predicted coreceptor usage based on V3 loop sequence in paired PBMC and plasma samples. Virus Res. 2007;130:34–42.

JOURNAL OF VIROLOGY, Nov. 2010, p. 11849–11857 Vol. 84, No. 22
0022-538X/10/$12.00 doi:10.1128/JVI.01464-10

Novel Immunodominant Peptide Presentation Strategy: a Featured HLA-A*2402-Restricted Cytotoxic T-Lymphocyte Epitope Stabilized by Intrachain Hydrogen Bonds from Severe Acute Respiratory Syndrome Coronavirus Nucleocapsid Protein▽†

Jun Liu,[1,2,3]‡ Peng Wu,[4]‡ Feng Gao,[5] Jianxun Qi,[1,2] Ai Kawana-Tachikawa,[6] Jing Xie,[4] Christopher J. Vavricka,[1] Aikichi Iwamoto,[6,7] Taisheng Li,[4]* and George F. Gao[1,2,3,8]*

CAS Key Laboratory of Pathogenic Microbiology and Immunology, Institute of Microbiology, Chinese Academy of Sciences (CAS), Beijing 100101, People's Republic of China[1]; China-Japan Joint Laboratory of Molecular Immunology and Molecular Microbiology, Institute of Microbiology, Chinese Academy of Sciences, Beijing 100101, People's Republic of China[2]; College of Life Sciences, Graduate University, Chinese Academy of Sciences, Beijing 100049, People's Republic of China[3]; Department of Infectious Diseases, Peking Union Medical College Hospital, Chinese Academy of Medical Sciences, Beijing 100730, People's Republic of China[4]; Institute of Biophysics (IBP), Chinese Academy of Sciences, Beijing 100101, China[5]; Division of Infectious Diseases, Advanced Clinical Research Center, Department of Infectious Diseases and Applied Immunology, Research Hospital, University of Tokyo, Minato-ku, 108-8639 Tokyo, Japan[6]; Institute of Medical Science, University of Tokyo, Minato-ku, 108-8639 Tokyo, Japan[7]; and Beijing Institutes of Life Science, Chinese Academy of Sciences, Beijing 100101, People's Republic of China[8]

Received 13 July 2010/Accepted 3 September 2010

Antigenic peptides recognized by virus-specific cytotoxic T lymphocytes (CTLs) are presented by major histocompatibility complex (MHC; or human leukocyte antigen [HLA] in humans) molecules, and the peptide selection and presentation strategy of the host has been studied to guide our understanding of cellular immunity and vaccine development. Here, a severe acute respiratory syndrome coronavirus (SARS-CoV) nucleocapsid (N) protein-derived CTL epitope, N1 (QFKDNVILL), restricted by HLA-A*2402 was identified by a series of *in vitro* studies, including a computer-assisted algorithm for prediction, stabilization of the peptide by co-refolding with HLA-A*2402 heavy chain and β_2-microglobulin (β_2m), and T2-A24 cell binding. Consequently, the antigenicity of the peptide was confirmed by enzyme-linked immunospot (ELISPOT), proliferation assays, and HLA-peptide complex tetramer staining using peripheral blood mononuclear cells (PBMCs) from donors who had recovered from SARS donors. Furthermore, the crystal structure of HLA-A*2402 complexed with peptide N1 was determined, and the featured peptide was characterized with two unexpected intrachain hydrogen bonds which augment the central residues to bulge out of the binding groove. This may contribute to the T-cell receptor (TCR) interaction, showing a host immunodominant peptide presentation strategy. Meanwhile, a rapid and efficient strategy is presented for the determination of naturally presented CTL epitopes in the context of given HLA alleles of interest from long immunogenic overlapping peptides.

In 2003, severe and acute respiratory syndrome (SARS), emerging from China, caused a global outbreak, affecting 29 countries, with over 8,000 human cases and greater than 800 deaths (5, 9, 24, 33, 37). Thanks to the unprecedented global collaboration coordinated by the WHO, SARS coronavirus (SARS-CoV), a novel member of *Coronaviridae* family, was rapidly confirmed to be the etiological agent for the SARS epidemic (36). Soon after the identification of the causative agent, SARS was controlled and then quickly announced to be conquered through international cooperation on epidemiological processes (9). However, the role that human immunity played in the clearance of SARS-CoV and whether the memory immunity will persist for the potential reemergence of SARS are not yet well understood.

In viral infections, $CD8^+$ cytotoxic T lymphocytes (CTLs) are essential to the control of infectious disease. Virus-specific $CD8^+$ T cells recognize peptides which have 8 to 11 amino acids, in most cases presented by major histocompatibility complex (MHC) class I molecules. However, identification of virus-specific $CD8^+$ T-cell epitopes remains a complicated and time-consuming process. Various strategies have been developed to define CTL epitopes so far. One of the most common practices to determine immunodominant CTL epitopes on a large scale is based on screening and functional analysis of overlapping 15- to 20-mer peptides covering an entire viral proteome or a given set of immunogenic proteins (19, 23, 32). However, peptides identified through this method are too long to be naturally processed CTL epitopes, and the definition of MHC class I restriction of these peptides still requires further

* Corresponding author. Mailing address for G. F. Gao: CAS Key Laboratory of Pathogenic Microbiology and Immunology, Institute of Microbiology, Chinese Academy of Sciences, No. 1 Beichen West Road, Chaoyang District, Beijing 100101, People's Republic of China. Phone: (86)10-64807688. Fax: (86) 10-64807882. E-mail: gaof@im.ac.cn. Mailing address for Taisheng Li: Department of Infectious Diseases, Peking Union Medical College Hospital, Chinese Academy of Medical Sciences, Beijing 100730, People's Republic of China. Phone and fax: (86) 10 -65295086. E-mail: litsh@263.net.

‡ J. Liu and P. Wu contributed equally to this work.

▽ Published ahead of print on 15 September 2010.

† The authors have paid a fee to allow immediate free access to this article.

TABLE 1. Characteristics of the peptides used in this study

Name	Derived protein	Positions	Sequence[a]	Score[b]
N1	SARS-CoV N protein	346–354	QFKDNVILL	19
NC9585	SARS-CoV N protein	338–354	IKLDDKDP**QFKDNVILL**	NA[c]
NC9586	SARS-CoV N protein	346–363	**QFKDNVILL**NKHIDAYKT	NA
Nef138-10[d]	HIV Nef protein	138–147	RYPLTFGWCF	22
B35-18[e]	HIV Pol protein	587–596	EPIVGAETFY	2
VYG[f]	Human telomerase	461–469	VYGFVRACL	23

[a] Boldface letters indicate peptide N1 within the peptides NC9585 and NC9586 (21).
[b] Estimated binding affinity to HLA-A*2402 calculated through the website http://www.syfpeithi.de/ (35).
[c] NA, scoring for peptides other than the nonamer and decamer to bind to HLA-A*2402 is not available.
[d] Nef138-10 was used as a positive control in the T2-A24 cell binding assay (11).
[e] B35-18 was used as a negative control in the T2-A24 cell binding assay (42).
[f] VYG was the peptide from the first peptide/HLA-A24 structure (7).

analysis. Rapid and efficient strategies should be developed for the determination of naturally presented CTL epitopes in the context of any given HLA allele of interest. Furthermore, no other HLA alleles except HLA-A2-restricted CTL epitopes have been reported for SARS-CoV-derived proteins (16, 22, 31, 43, 46, 47, 49). This is primarily because of the limitation of the experimental methods for the other HLA alleles. HLA-A24 is one of the most common HLA-A alleles throughout the world, especially in East Asia, where SARS-CoV emerged, second only to HLA-A2 (30). The development of a fast and valid method to screen and identify HLA-A24-restricted epitopes would greatly contribute to the understanding of the specific CTL epitope-stimulated response and widen the application of the epitope-based vaccine among a more universal population (17). A genomewide scanning of HLA binding peptides from SARS-CoV has been performed by Sylvester-Hvid and colleagues, through which dozens of peptides with major HLA supertypes, including HLA-A24 binding capability, have been identified (41).

There are strong indications that different peptide ligands, such as peptides with distinct immunodominance, can elicit a diverse specific T-cell repertoire, and even subtle changes in the same peptide can have a profound effect on the response (25, 44). Furthermore, a broader T-cell receptor (TCR) repertoire to a virus-specific peptide–MHC complex can keep the host resistant to the virus and limit the emergence of virus immune-escape mutants (29, 34, 38). Recent studies have demonstrated that the diversity of the selected TCR repertoire (designated as T-cell receptor bias) is clearly influenced by the conformational characteristics of the bound peptide in the MHC groove. Peptides with a flat, featureless surface when presented by MHC generate only limited TCR diversity in a mature repertoire, while featured peptides with exposed residues (without extreme bulges) protruding outside the pMHC landscapes are rather associated with the more diverse T-cell repertoire (15, 28, 39, 44, 45). Therefore, being able to determine the binding features of a peptide to MHC and describe the peptide-MHC topology will help us understand the immunodominance of a given peptide and demonstrate the peptide presentation strategy of the host.

Structural proteins of SARS-CoV, such as spike, membrane, and nucleocapsid (N), have been demonstrated as factors of the antigenicity of the virus, as compared with the nonstructural proteins (12, 20). Coronavirus nucleocapsid (N) protein is a highly phosphorylated protein which not only is responsible for construction of the ribonucleoprotein complex by interacting with the viral genome and regulating the synthesis of viral RNA and protein, but also serves as a potent immunogen that induces humoral and cellular immunity (13, 14, 26, 48). The $CD8^+$ T-cell epitopes derived from SARS-CoV N protein defined so far mainly cluster in two major immunogenic regions (4, 21, 23, 31, 32, 43). One of them, residues 219 to 235, comprises most of the N protein-derived minimal CTL epitopes identified so far—N220-228, N223-231, N227-235, etc.—all of which are HLA-A*0201 restricted (4, 43). The other region, residues 331 to 365, also includes high-immunogenicity peptides that can induce memory T-lymphocyte responses against SARS-CoV (21, 23, 32). However, until now, no minimal CTL epitope with a given HLA allele restriction has been investigated in this region.

Here, based on previously defined immunogenic regions derived from SARS-CoV N protein (21), we identified an HLA-A*2402-restricted epitope, N1 (residues 346 to 354), in the region through a distinct strategy using structural and functional approaches. The binding affinity with HLA-A*2402 molecules and the cellular immunogenicity of the peptide were demonstrated in a series of assays. The X-ray crystal structure of HLA-A*2402 complexed with peptide N1 has shown a novel host strategy to present an immunodominant CTL epitope by intrachain hydrogen bond as a featured epitope.

MATERIALS AND METHODS

Peptide prediction and synthesis. To identify the potential HLA-A*2402-binding peptides within SARS-CoV N protein (GenBank accession no. AY278741), a computer-based program was applied by access through the website of SYFPEITHI (35). One peptide with the sequence positions N346 to 354 (QFKDNVILL) was predicted with high binding affinity to HLA-A*2402. This peptide, later termed N1, happened to be located in one of the highest-immunogenicity regions of the SARS-CoV N protein, which is between amino acids 330 and 354 (21). N1 was synthesized, and the purity was determined as ~95% by analytical high-performance liquid chromatography (HPLC) and mass spectrometry (Scilight-Peptide, Inc.). HLA-A*2402-binding peptide Nef138-10 (RYPLTFGWCF) (11), derived from HIV Nef protein, and HLA-B*3501-restricted peptide B35-18 (EPIVGAETFY) (42), derived from HIV Pol protein, were synthesized and used as control peptides. The peptides used in the following assays are listed in Table 1.

Refolding of peptides with HLA-A*2402 heavy chain and β_2m. HLA-A*2402 heavy chain and β_2-microglobulin (β_2m) were overexpressed as recombinant proteins in *Escherichia coli* and subsequently *in vitro* refolded and assembled in the presence of high concentration of peptide or without any peptide. Generally, the refolding buffer was 250 ml and the molar ratio of heavy chain, β_2m, and peptide was 1:1:2. After sufficient time for protein refolding, the buffer was

TABLE 2. Characteristics of the subjects used in this study

Patient group	ID	Age (yr)	Sex	HLA allele			
				HLA-A		HLA-B	
HLA-A24$^+$	Patient 1	28	Female	A24	A3	B60	B27
	Patient 2	35	Male	A24	A11	B62	B13
	Patient 3	43	Male	A24	A2	B46	B13
HLA-A24$^-$	Patient 4	33	Female	A2	A2	B60	B67
HLA-A24$^+$ healthy donors	Donor 1	30	Male	A24	A11	B60	B60
	Donor 2	41	Female	A24	A3	B7	B13

concentrated and analyzed by Superdex 200 10/300 GL gel-filtration chromatography (GE Healthcare).

MHC stabilization assay with T2-A24 cells. MHC stabilization assays were performed by previously described methods (11). Briefly, T2-A24 cells were incubated at 26°C for 16 h, and then 2×10^5 cells were incubated with peptides at concentrations from 10^{-8} to 10^{-4} mM for 1 h at 4°C. After incubation for 3 h at 37°C, the cells were stained with anti-HLA-A24 monoclonal antibody (MAb), A11.1 M (10), and an R-phycoerythrin (RPE)-conjugated $F(ab')_2$ fragment of anti-mouse immunoglobulin (Dako). The mean fluorescence intensity was measured by FACSCalibur (Becton Dickinson).

X-ray crystallography, structure determination, and refinement. HLA-A*2402/peptide complexes were refolded by the gradual-dilution method as described above (6, 7, 40). Subsequently, the remaining soluble portion of the complex was concentrated and purified by Superdex 200 10/300 GL gel filtration chromatography and Resource-Q anion-exchange chromatography (GE Healthcare). Crystals were grown by the hanging-drop vapor diffusion method at 4°C. Single HLA- A*2402/N1 crystals were grown at a final concentration of 20 mg/ml in a mixture of 0.2 M ammonium sulfate, 0.1 M Tris (pH 8.9), and 25% (wt/vol) polyethylene glycol 3350. Over the course of 3 days by microseeding, the crystals grew to the maximal size of 400 by 80 by 80 μm. For cryoprotection, crystals were transferred to reservoir solutions containing 20% glycerol. Crystallographic data were collected at 100K in house on a Rigaku MicroMax007 rotating-anode X-ray generator operated at 40 kV and 20 mA (Cu Kα; λ = 1.5418 Å) equipped with an R-AXIS VII++ image-plate detector. Data were indexed and scaled using DENZO and the HKL2000 software package.

The structure was determined using molecular replacement with the program CNS (3). The search model was PDB (Protein Data Bank) code 2BCK with water coordinates omitted (7). Extensive model building was performed by hand using COOT (8) and with restrained refinement using REFMAC5. The further rounds of refinement were performed using the phenix refine program implemented in the PHENIX package with isotropic ADP refinement and bulk solvent modeling (1). The stereochemical quality of the final model was assessed with the program PROCHECK (18). Figure 3 and Fig. 4 were generated using PyMOL (http://www.pymol.org/).

PBMCs from donors. During the 2003 SARS epidemic in Beijing, China, we enrolled and sequentially followed up SARS patients who were diagnosed and recovered from SARS-CoV infection, according to the clinical criteria released by the World Health Organization (WHO; http://www.who.int/csr/sars/casedefinition/en). The purpose and performance of the study were fully explained to all participants from the Beijing Union Medical College Hospital, Beijing, China. Collection of peripheral blood mononuclear cell (PBMC) samples was authorized by the Hospital Ethics Review Committee. Standard serologic HLA typing was performed with peripheral blood from the donors. PBMC samples from three HLA-A24$^+$ patients and from one HLA-A24$^-$ patient who had recovered from SARS were selected. Two HLA-A24$^+$ healthy donors' PBMCs were used as a control (Table 2). The frequencies of HLA-A24 expression in patients who had recovered from SARS and healthy donors were 12.5% and 20%, respectively.

***In vitro* stimulation and culture of PBMCs.** The cells were thawed and incubated with 10 μM peptides in RPMI 1640 containing 10% fetal calf serum (FCS) at 37°C with 5% CO_2 at a cell density of 2×10^6/ml in a 24-well culture plate, and on day 3, 20 U/ml recombinant human IL-2 (rhIL-2) was added to the medium. Half of the medium was changed on day 4 and day 7 with supplementation with 20 U/ml rhIL-2. On day 9, cells were harvested and tested for the presence of peptide-specific CD8$^+$ T cells by enzyme-linked immunospot (ELISPOT) assay and tetramer staining.

ELISPOT assay. The antigen-specific response of T lymphocytes induced by peptides was measured by the use of a gamma interferon (IFN-γ) ELISPOT set (U-CyTech). Briefly, a 96-well ELISPOT plate membrane was preincubated with diluted anti-IFN-γ coating antibody overnight at 4°C. The next day, wells were washed with phosphate-buffered saline (PBS) and blocked with diluted blocking solution for 1 h at 37°C. PBMCs from donors were incubated in microwells (1×10^5 to 3×10^5/well) along with stimulating peptides (20 μM) or phytohemagglutinin (PHA) as a positive control of nonspecific stimulation for 24 h at 37°C with 5% CO_2. Cells incubated without a stimulator were employed as a negative control that produced less than five spots per well in 90% of the experiments. Subsequently the cells were removed, and the plate was processed in turn with biotinylated detection antibodies, streptavidin-horseradish peroxidase (HRP) conjugate, and substrate 3-amino-9-ethylcarbazole (AEC). Development of colored spots was stopped by thorough rinsing with demineralized water. The results were analyzed using an automatic ELISPOT reader.

Tetramer production and staining. HLA-peptide tetramers were produced as described previously (49). Briefly, expression of the HLA heavy chain was limited to the extracellular domain (residues 1 to 276), and the C terminus of the α3 domain was modified by the addition of a substrate sequence for the biotinylating enzyme BirA. Large amounts of soluble pHLA complexes were generated by refolding. *In vitro* biotinylation of the pHLA complexes was achieved by incubating the sample with the biotin protein ligase BirA (recombinant expressed) and other D-biotin and ATP (Avidity). The samples were purified again through gel filtration before the multimerization by using streptavidin conjugated with phycoerythrin (PE) (Sigma). Cells from the subjects were stained with tetramer (0.05 μg/μl), PE-Cy5-labeled anti-CD3, and fluorescein isothiocyanate (FITC)-conjugated anti-CD8 antibody. The cells were then resuspended in 400 μl staining buffer and analyzed by flow cytometry immediately.

Proliferation assay with CFSE staining. PBMCs were thawed and resuspended in RPMI 1640 medium at 2.5×10^6/ml. Cells were stained with carboxyfluorescein isothiocyanate (CFSE) at 1 μg/ml for 25 min at 37°C in the dark. Cells were washed three times with cold RPMI 1640 medium containing 10% FBS, stimulated with 10 μg/ml peptide and 25 ng/ml IL-7, and incubated in the dark. IL-2 (20 U/ml) was added on day 3. On day 7, cells were washed and fluorescence was detected by flow cytometry. p24 antigen from HIV was used as a negative control.

Protein structure accession number. The accession number of the structure of N1 pMHC in the Protein Data Bank is 3I6L.

RESULTS

Analysis of the potential HLA-A24-restricted epitopes in SARS N protein. Since no HLA allele-restricted epitopes other than for HLA-A2 have been identified throughout the proteome of SARS so far, we are interested in the definition of HLA-A24-restricted epitopes derived from the SARS-CoV N protein, which can play a critical role in cellular immunity in HLA-A24$^+$ patients against SARS-CoV. We predicted the potential HLA-A*2402-restricted epitopes derived from the sequence of N protein through computer analysis. It was found that the peptide with the highest score is nonamer peptide N1 (QFKDNVILL), covering the residues from positions 346 to 354 of the N protein. Further analysis indicated that peptide

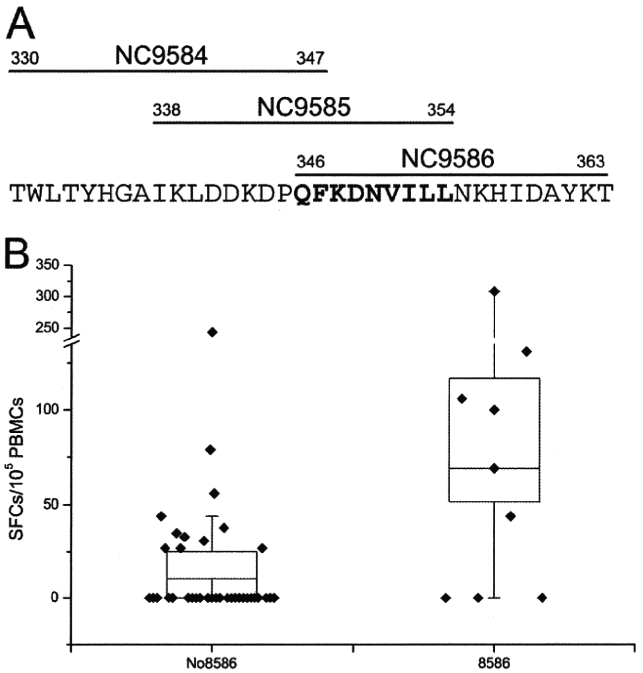

FIG. 1. HLA class I restriction of the immunogenic region within SARS N protein. (A). The sequence of amino acid residues 330 to 363 along the N protein. N330 to N354 was an immunogenic region within SARS N protein identified in a previous study (21). Peptide N1 (N346 to N354), which is shown in boldface, is included by both peptide NC9585 (N338 to N354) and NC9586 (N346 to N363). (B) Data reanalysis of the ELISPOT assays performed with three HLA-A24$^+$ donors recovered from SARS donors (patient 1, patient 2, and patient 3 in the ID [identification] column in Table 2). The entry 8586 represents the peptide pools NX6, NY7, and NY8, which contain peptides NC9585 and NC9586. Meanwhile, No8586 represents the other peptide pools that do not include these two peptides. The top and bottom of each rectangular box denote the standard error (SE), with the median shown inside the box. Horizontal bars extending from each box represent the 90th and 10th percentiles. Rhombus dots indicate the specific CD8$^+$ T-cell responses of the recovered individual donors stimulated by different peptide pools. One dot represents the average response of one individual donor reacting to one of the peptide pools from two independent tests. The total number of dots for entry 8586 is 9, which was calculated as follows: 3 peptide pools × 3 HLA-A24$^+$ donors. There are 12 pools which do not include these two peptides; therefore, the number of dots for No8586 is 36, which was calculated as follows: 12 peptide pools × 3 HLA-A24$^+$ donors. Details for peptide pools can be found in reference 21.

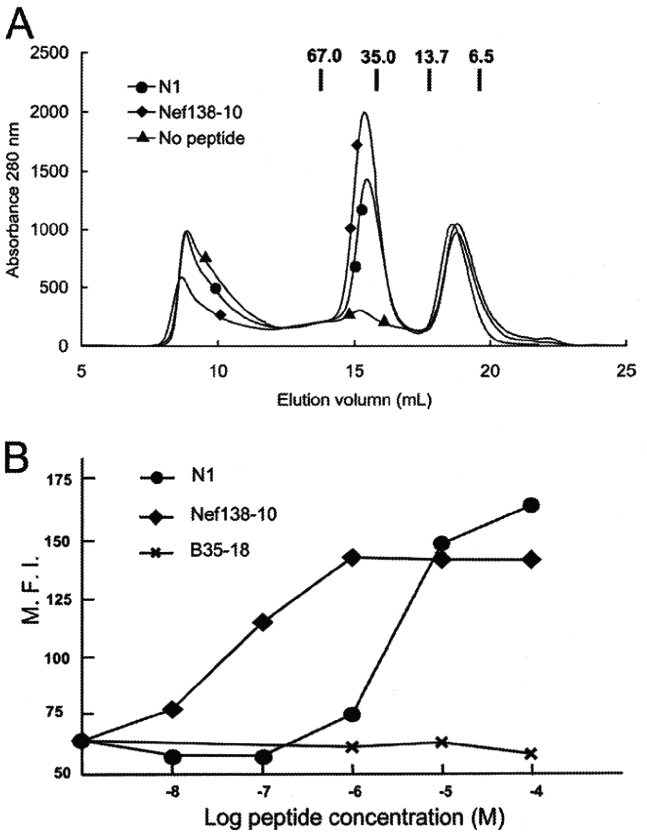

FIG. 2. Binding affinity of peptide N1 to the HLA-A*2402 molecule. (A) *In vitro* refolding of HLA-A*2402 heavy chain and β_2m with N1. As compared to the much lower peak of refolding without any peptide, N1 together with the positive control peptide Nef138-10 could help the HLA-A*2402 complexes refold. The peaks of the complexes with the expected molecular mass of 45 kDa were eluted at the estimated volume of 16 ml on a Superdex 200 column (GE Healthcare). The profile is marked with the approximate positions of the molecular mass standards of 67.0, 35.0, 13.7, and 6.5 kDa. (B) Peptide binding to HLA-A*2402 was quantified by using a T2-A24 stabilization assay. M.F.I., mean fluorescence intensity. These results are representative of three independent experiments.

N1 exists in one of the previously defined two immunodominant regions: positions 330 to 354 (21), which contains potential CTL epitopes in the N protein, as demonstrated in our previous study (Fig. 1A).

Peptide N1 is included in the overlapping peptides NC9585 (N338 to N354) and NC9586 (N346 to N363), and peptide pools containing these two overlapping peptides are NX6, NY7, and NY8 (21). A second analysis of the ELISPOT data shows that, with regard to HLA-A24$^+$ donors who had recovered from SARS, these three peptide pools stimulated distinct CTL epitope-stimulated responses in donors who had recovered from SARS compared to other peptide pools ($P < 0.01$) (Fig. 1B). Taking all these findings into consideration, region N338 to N363 may contain HLA-A24-restricted CTL epitopes, and peptide N1 acts as the candidate with the most potential among them.

Binding affinity to HLA-A*2402. Peptide N1 was selected and synthesized for further analysis. To evaluate the binding efficiency of the peptide to the HLA-A*2402 molecule, we performed a peptide-induced refolding assay of the HLA-A*2402 heavy chain and β_2m *in vitro* (Fig. 2A). Peptide N1 could conspicuously help HLA-A*2402 heavy chain and β_2m refold and form a stable complex. Peptide Nef138-10 acted as the positive control and presented a high binding capability to HLA-A*2402 molecule. HLA-A*2402 heavy chain and β_2m could not form the MHC complexes without the presence of any peptide.

To further determine the binding affinity of these two peptides to the HLA-A*2402 molecule at cellular level, we manipulated an MHC stabilization assay by using T2-A24 cells (Fig. 2B). Although, compared to the positive control peptide Nef138-10, peptide N1 had a lower binding avidity to HLA-A24, N1 distinctly increased HLA-A24 expression on the cell

TABLE 3. X-ray data and refinement statistics

Parameter	HLA-A*2402/N1 result(s)
Data collection statistics	
Space group	P212121
Dimensions, *a*, *b*, *c* (Å)	70.4, 85.8, 92.2
Angles, α, β, γ (°)	90.0, 90.0, 90.0
Resolution (Å)	2.4 (2.49–2.40)[a]
Total no. of reflections	149,410
No. of unique reflections	22,272
Completeness (%)	98.6 (97.5)
I/σ	40.7 (6.2)
R_{merge} (%)[b]	9.9 (38.7)
Refinement statistics	
Resolution (Å)	2.4
R_{work} (%)[c]	21.3
R_{free} (%)	28.4
Average B-factor (Å^2)	43.5
Root mean square deviation from the ideal	
Bond length (Å)	0.013
Bond angle (°)	1.443

[a] The numbers in parentheses refer to the number of structure factors used in the measurements.

[b] $R_{merge} = \Sigma_{hkl}\Sigma_i|I_i - \langle I\rangle|\Sigma_{hkl}\Sigma_i I_i$, where I_i is the observed intensity and $\langle I\rangle$ is the average intensity of multiple observations of symmetry-related reflections.

[c] $R = \Sigma_{hkl}||F_{obs}| - k|F_{cal}||/\Sigma_{hkl}|F_{obs}|$, where R_{free} is calculated for a randomly chosen 5% of reflections and R_{work} is calculated for the remaining 95% of reflections used for structure refinement.

surface, indicating that it bound and stabilized the HLA complexes on the cell surface. Negative control peptide B35-18 was determined to have no affinity of binding to HLA-A24, even at a high concentration in the assay.

Overview of HLA-A*2402/N1 structure. The crystal structure of the HLA-A*2402/N1 complex has been determined to a resolution of 2.4 Å (Table 3). The only HLA-A24 structure released in the Protein Data Bank to date is that of HLA-A*2402/VYG (2BCK) with a resolution of 2.8 Å. The higher resolution of HLA-A*2402/N1 complex allows for a more detailed interpretation of the peptide binding of HLA-A24 and rigorous incorporation of additional water molecules.

The HLA-A*2402 structure in the HLA-A*2402/N1 complex is very similar to the HLA-A*2402/VYG structure, with root mean square differences (RMSDs) of 0.771 Å and 0.272 Å for the heavy chain and β_2m, respectively. The unambiguous electron density for the peptide ligand N1 clearly shows the main chain conformation of the peptide and the orientations of the residue side chains. As seen in the previous HLA-A*2402 structure, peptide positions 2 and 9 are major anchors, with F2 deeply buried in the B pocket and L9 in the F pocket (Fig. 3). Comparison of the B pockets in the two structures indicates that the changing of primary anchor residue from Y to F does not induce position changes of the residues in peptide binding pocket B. The backbones of the residues forming the B pockets (Y7, S9, A24, V25, V34, M44, K65, V67, and Y99 of HLA-A24 heavy chain) of the two structures superimpose to an RMSD of 0.249 Å. However, the structure of HLA-A*2402/N1 contains phenylalanine, whereas HLA-A*2402/VYG contains a tyrosine and therefore lacks a hydrogen bond with His 70 of the heavy chain, the only observed discrimination between the two major anchor residues in position 2 of HLA-A24 binding peptides. The secondary anchor of N1 is quite different from that of peptide VYG. Position 3 of N1 is a secondary anchor, with K3 inserted into the D pocket, while V5 of peptide VYG at position 5 participates as the secondary anchor residue.

Conformational features of N1 presented by HLA-A*2402. The main chain of the central region of N1 exists in a unique conformation which can be described as "A" shaped. This is quite different from VYG, which adopts an "M"-shaped conformation. For VYG, the prominently exposed residues are F4 and R6, which form the two tops of the "M." The secondary anchor residue V5, which forms the dip in the "M," secures the peptide in the groove. However, for N1, the three adjacent residues D4, N5, and V6 of the central region bulge out of the

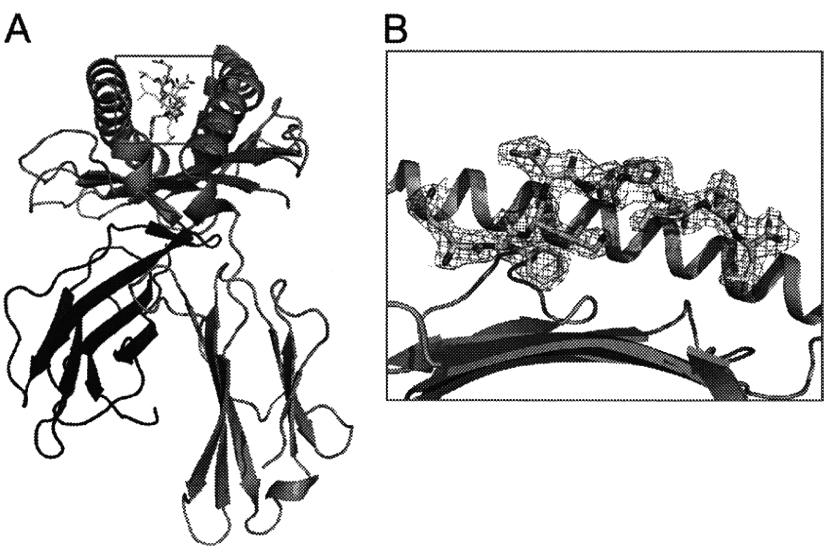

FIG. 3. Structure of the HLA-A*2402/N1 complex. (A) Overview of the structure of HLA-A*2402/N1. (B) The electron density of N1 shows the conformation of the peptide with the second residue of N-terminus F2 and the C-terminus residue L9 to anchor in the HLA groove. Shown here are final 2Fo-Fc-stimulated annealing omit maps contoured at 1.0 σ.

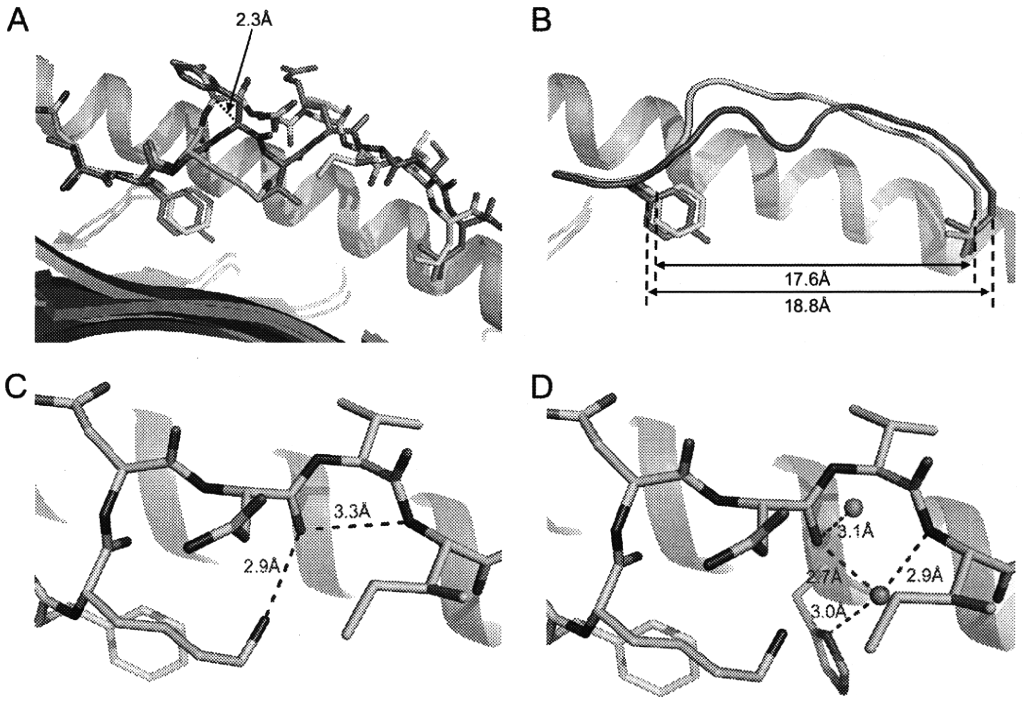

FIG. 4. Conformational features of peptide N1 in the binding groove of HLA-A*2402. (A) D4, N5, and V6 in the middle part of peptide N1 (yellow) bulge out of the peptide binding groove, with the backbone of the three residues rising about 2.3 Å compared to peptide VYG (pink; PDB ID no. 2BCK). (B) The distance between β-carbons of the residues at position 2 and position 9 of N1 (yellow) and VYG (pink) shows the whole length of N1 adopts a more bulged conformation. (C) Two intrachain hydrogen bonds are formed between K3 and N5 and also between N5 and I7, respectively. The side chains of residues D4 and V6, between the two hydrogen bonds, protrude out of the HLA groove and may play a dominant role in the TCR-MHC docking. (D) Central residues of N1 interact with α-helix of HLA-A*2402 through two water molecules.

HLA-A24 surface for potential TCR docking. The distinct "A"-shaped conformation raised the backbone of the central region residues of peptide N1 about 2.3 Å compared to VYG (the distance between α-C of D4 of N1 and F4 of VYG) (Fig. 4A). Although the side chains of D4 and V6 of N1 are quite shorter than the corresponding residues in VYG, F4 and R6, the main chain ascending from N1 enables the side chain ends of D4 and V6 to reach out to an incredible level from the peptide binding groove of HLA. Especially, the side chain of D4 of N1 is raised to the same level as F4 of VYG, which may be helpful for TCR docking. The distance between β-carbons of the residues at position 2 and position 9 of N1 is shorter than that of VYG. The distance between β-carbons of F2 and L9 for N1 is 17.6 Å, and for Y2 and L9 of VYG, it is 18.8 Å (Fig. 4B). This phenomenon demonstrates that, not only the central region, but also the overall main chain of N1 adopts a more bulged conformation, while that of peptide VYG is a relatively extended one. This may also contribute to the protruding extent of the residues at the central region of N1, which can be defined to have the featured characteristic when presented by HLA-A24.

Further analysis of the HLA-A*2402/N1 structure indicated a distinct structure of the N1 peptide in the groove may facilitate the formation of the exclusive conformation of peptide N1. First, the presence of two intrachain hydrogen bonds in the ligand peptide is rarely found among the HLA ligand peptides. The carbonyl oxygen atom of N5 shares the hydrogen atom with the amino group of the side chain of K3 and the amino nitrogen of I7, respectively, to form two intrachain hydrogen bonds (Fig. 4C). These two intrachain hydrogen bonds act as the transverse line in the "A"-shaped conformation of N1 to help the rigid conformation become more stable. Second, the vacuous space formed by the stretching of the two hydrogen bonds is occupied by two water molecules. Residues N5 and I7 interact with these water molecules and are fixed to the α1-helix of HLA-A24 (Fig. 4D). No water molecules are found under the main chain of VYG in the HLA-A*2402/VYG structure.

Investigation of the immunogenicity of N1 with PBMCs of HLA-A24$^+$ in donors recovered from SARS. To determine the immunogenicity of peptide N1, PBMCs of HLA-A24$^+$ donors recovered from SARS were stimulated for 9 days in the presence of peptide N1. The induction of IFN-γ was revealed by the ELISPOT assays with the peptide N1 and two overlapping peptides NC9585 and NC9586 as stimulators. As shown in Fig. 5, N1 significantly elicited specific IFN-γ-producing CD8$^+$ T cells from the PBMCs of HLA-A24$^+$ donors recovered from SARS in comparison to the HLA-A24$^-$ donors recovered from SARS and HLA-A24$^+$ healthy controls (60.5 ± 20.8 versus 6.9 ± 5.4 and 1.3 ± 0.9 spot-forming cells (SFC)/10^5 PBMCs; $P < 0.01$). The overlapping peptides, NC9585 and NC9586, also possessed the ability to stimulate specific IFN-γ production in the HLA-A24$^+$ donors recovered from SARS in comparison to the negative controls ($P < 0.01$). This indicated that these two peptides (which cover the N1 peptide) possessed cross-immunogenicity with peptide N1.

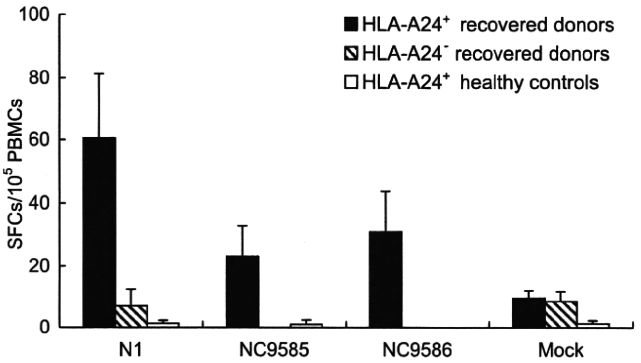

FIG. 5. Detection of peptide N1-specific $CD8^+$ T cells in PBMCs of $HLA\text{-}A24^+$ donors recovered from SARS by ELISPOT. The mean numbers of SFCs in 10^5 splenocytes are represented with bars as a measure of IFN-γ secretion from human PBMCs stimulated with peptides. The PBMC samples from two $HLA\text{-}A24^+$ donors recovered from SARS were thawed and manipulated in ELISPOT assays.

Consequently, the HLA-A*2402/N1 tetramer was prepared and used to confirm the frequency of N1-specific $CD8^+$ T cells. PBMCs from $HLA\text{-}A24^+$ donors recovered from SARS and $HLA\text{-}A24^+$ healthy donors were stained with HLA-A*2402/N1 tetramer after 9-day incubation with N1 and rhIL-2. An average of 0.2% of $CD8^+$ T cells were determined as N1-specific $CD8^+$ T cells from PBMCs of the $HLA\text{-}A24^+$ donors recovered from SARS. In contrast, no N1-specific T cells were detectable from the PBMCs of all tested $HLA\text{-}A24^+$ healthy controls (Fig. 6A).

In the proliferation assay, peptide N1 significantly induced proliferation responses among $HLA\text{-}A24^+$ donors recovered from SARS as measured by CFSE dilution (Fig. 6B), rather than $HLA\text{-}A24^+$ healthy controls (19% versus 4%). Furthermore, when PBMCs were stimulated with negative control HIV p24 protein, the proliferation rates showed no significant difference between $HLA\text{-}A24^+$ donors recovered from SARS and $HLA\text{-}A24^+$ healthy controls (1% versus 2%).

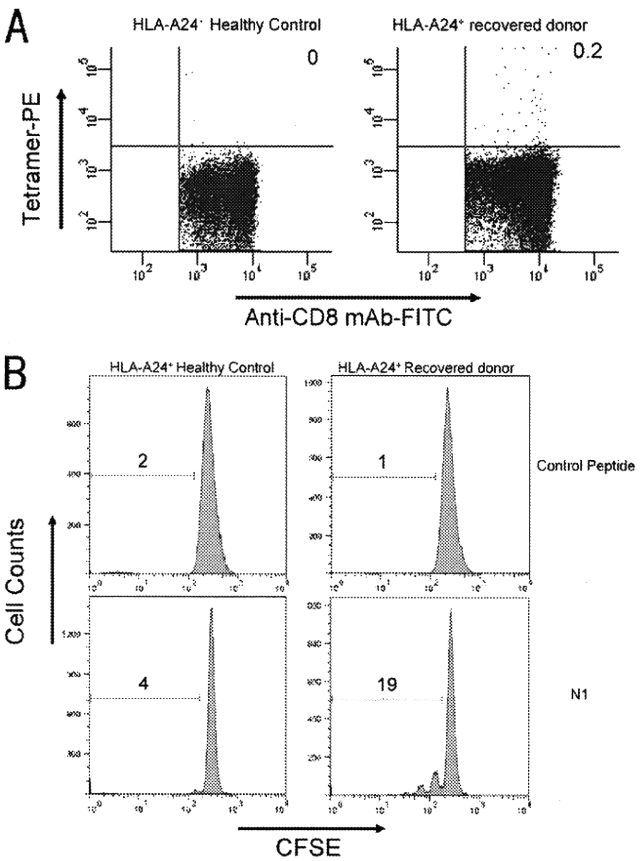

FIG. 6. Identification of the immunogenicity of N1 by fluorescence staining and flow cytometry. (A) In tetramer staining, N1-specific $CD8^+$ T cells were measured from N1-stimulated PBMCs of an $HLA\text{-}A24^+$ donor recovered from SARS (patient 1) and an $HLA\text{-}A24^+$ healthy donor (donor 1), using the PE-labeled HLA-A*2402/N1 tetramer along with PE-Cy5-labeled anti-CD3 and FITC-labeled anti-CD8 MAbs for cell staining. (B) PBMCs from an $HLA\text{-}A24^+$ donor recovered from SARS (patient 3) and an $HLA\text{-}A24^+$ healthy donor (donor 2) were stained with 1 μM CFSE and stimulated by peptides for 7 days. Panels represent percentages of cells that have undergone divisions.

DISCUSSION

Antigenic peptides recognized by virus-specific CTLs are not only useful tools for studying cellular immunity against virus, but also potential reagents for development of immunotherapy. However, the identification of novel CTL epitopes is generally time-consuming and labor-intensive. A large number of 15- to 20-mer peptides with determined immunogenicity for CTLs against viruses as SARS-CoV and influenza virus have been identified without awareness of the HLA allele (19, 21). The immunogenicities of the peptides are evaluated by immunological approaches like cytokine-specific ELISPOT or flow cytometry (23, 32). However, to identify naturally presented optimal epitopes within these long peptides and the HLA allele restriction of these peptides, a large amount of work is still required (2, 27). In a previous study, we have identified two long immunogenic domains within the sequence of SARS-CoV N protein, using the overlapping 15- to 18-mer peptides (21). In this study, we illustrate an efficient and rapid strategy to define minimal natural CTL epitopes presented by a specific HLA allele, HLA-A*2402, while targeting long overlapping peptides. Peptide N1 derived from SARS-CoV N protein was identified as an immunodominant epitope with a featured conformation when binding to HLA-A*2402.

As a nonameric peptide, N1 has no residues with long side chains but shows an immunodominant featured character (21). There are common indications that featured peptides with exposed side chains can generate a more diverse T-cell repertoire than flat, featureless peptides (15, 28, 39, 44, 45). However, how would the "featureless" amino acid contents of N1 help the peptide become a featured epitope? Our study in this report shows that N1 takes use of a featured "A"-shaped conformation with the side chain of N5 in position 5 projecting out of the peptide binding groove, instead of acting as a middle, secondary anchoring residue (7). The side chains of the central region of N1 protrude to the same level as peptide VYG, which has the characteristic featured residues (7). Taking advantage of this strategy, HLA-A*2402/N1 represents a typical structural landscape for a featured peptide which may help to generate a more diverse T-cell repertoire. This intrachain hydro-

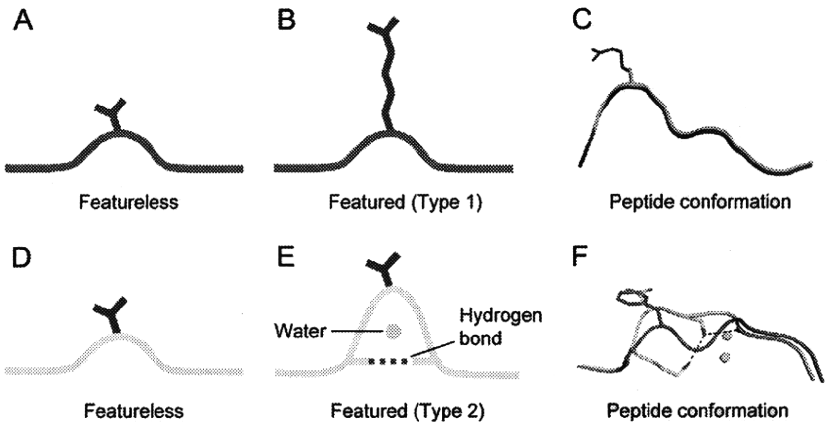

FIG. 7. Topology of the newly identified presentation strategy of featured peptides. Featureless peptides have a typical amino acid length (8 to 10 amino acids) but have few or no solvent-exposed residues with prominent side chains (A and D). The previously determined characteristic of featured peptide is defined as type 1 featured peptide (B). These peptides comprise solvent-exposed residues presenting prominent side chains for recognition by a diverse TCR repertoire (C). In this study, a new presentation strategy of featured peptides was identified (E). Peptide without solvent-exposed residue arches itself through intrachain hydrogen bonds and water molecules under the main chain of the peptide. Through this strategy, short side chains of peptide N1 (yellow) protrude to the level of solvent-exposed residues of peptide VYG (pink) and may be recognized by an immune T-cell repertoire of high diversity (F).

gen-bonding strategy of the host antigen presentation might represent a second type (type 2) of featured epitope in addition to the previously defined type with characteristic long-side chain residues (type 1) (44). This may help us to understand the peptide presentation strategy of the host: exposing the shorter side chain amino acid by making the middle region bulge through intrachain hydrogen bonds to make the peptide a featured epitope (Fig. 7).

The formation of the particular conformation of N1 may be partially due to the contrast of biochemical qualities between the residues in position 5 of peptide N1 and VYG. The D pocket of the HLA-A24 peptide binding groove is hydrophobic and can accommodate the side chain of valine from position 5 of VYG with higher hydrophobicity. In contrast, the side chain of asparagine in position 5 of N1 is repelled out of the D pocket because of the hydrophilicity of the asparagine. Exceptional intrachain hydrogen bonds and under-the-chain water molecules contribute to stabilize the conformation of the central region.

The newly identified peptide N1 (QFKDNVILL), which acts as a dominant epitope located in one of the immunogenic regions, residues 331 to 365 of N protein, could be used as a representative CTL antigen for detection of SARS-CoV-specific CTL epitope-stimulated response within the HLA-A24$^+$ donors recovered from SARS. In addition, it might be a candidate reagent for peptide vaccine development. The novel structure of HLA-A*2402 together with a pathogen-derived peptide in a higher resolution may expand our understanding of the peptide binding properties of HLA-A24 molecules and the strategy of the host to present immunodominant epitopes.

ACKNOWLEDGMENTS

This study was supported by the China National Grand S&T Special Project (2009ZX10004-305/201), the National Natural Science Foundation of China (NSFC; grant 81021003), Key International Science and Technology Cooperation Projects (2007DFC30240), and the National Basic Research Program (project 973, grant 2006CB504204) of the Ministry of Science and Technology of the People's Republic of China. The China-Japan Joint Laboratory of Molecular Immunology and Molecular Microbiology is, in part, supported by Japan MEXT (Ministry of Education, Culture, Sports, Science and Technology). J.L. is supported, partly for this project, by the Doctoral Candidate Innovation Research Support Program by Science & Technology Review (kjdb20090102-4). Christopher J. Vavricka is partially supported by the Fellowship for Young International Scientists of the Chinese Academy of Sciences (2009Y2BS2).

We thank Zhenying Liu from the Institute of Microbiology, Chinese Academy of Sciences, for excellent suggestions and technical assistance.

The authors declare they have no financial or commercial conflicts of interest. The funders of this study had no role in the study design, data collection and analysis, decision to publish, or preparation of the manuscript.

REFERENCES

1. **Adams, P. D., R. W. Grosse-Kunstleve, L. W. Hung, T. R. Ioerger, A. J. McCoy, N. W. Moriarty, R. J. Read, J. C. Sacchettini, N. K. Sauter, and T. C. Terwilliger.** 2002. PHENIX: building new software for automated crystallographic structure determination. Acta Crystallogr. D Biol. Crystallogr. **58:** 1948–1954.
2. **Bertoletti, A., F. V. Chisari, A. Penna, S. Guilhot, L. Galati, G. Missale, P. Fowler, H. J. Schlicht, A. Vitiello, R. C. Chesnut, F. Fiaccadori, and C. Ferrari.** 1993. Definition of a minimal optimal cytotoxic T-cell epitope within the hepatitis-B virus nucleocapsid protein. J. Virol. **67:**2376–2380.
3. **Brunger, A. T., P. D. Adams, G. M. Clore, W. L. DeLano, P. Gros, R. W. Grosse-Kunstleve, J. S. Jiang, J. Kuszewski, M. Nilges, N. S. Pannu, R. J. Read, L. M. Rice, T. Simonson, and G. L. Warren.** 1998. Crystallography & NMR system: a new software suite for macromolecular structure determination. Acta Crystallogr. D Biol. Crystallogr. **54:**905–921.
4. **Cheung, Y. K., S. C. Cheng, F. W. Sin, K. T. Chan, and Y. Xie.** 2007. Induction of T-cell response by a DNA vaccine encoding a novel HLA-A*0201 severe acute respiratory syndrome coronavirus epitope. Vaccine **25:**6070–6077.
5. **Chinese SARS Molecular Epidemiology Consortium.** 2004. Molecular evolution of the SARS coronavirus during the course of the SARS epidemic in China. Science **303:**1666–1669.
6. **Chu, F. L., Z. Y. Lou, Y. W. Chen, Y. W. Liu, B. Gao, L. L. Zong, A. H. Khan, J. I. Bell, Z. H. Rao, and G. F. Gao.** 2007. First glimpse of the peptide presentation by rhesus macaque MHC class I: crystal structures of Mamu-A*01 complexed with two immunogenic SIV epitopes and insights into CTL escape. J. Immunol. **178:**944–952.
7. **Cole, D. K., P. J. Rizkallah, F. Gao, N. I. Watson, J. M. Boulter, J. I. Bell, M. Sami, G. F. Gao, and B. K. Jakobsen.** 2006. Crystal structure of HLA-A*2402 complexed with a telomerase peptide. Eur. J. Immunol. **36:**170–179.
8. **Emsley, P., and K. Cowtan.** 2004. Coot: model-building tools for molecular graphics. Acta Crystallogr. D Biol. Crystallogr. **60:**2126–2132.
9. **Feng, Y. J., and G. F. Gao.** 2007. Towards our understanding of SARS-CoV,

an emerging and devastating but quickly conquered virus. Comp. Immunol. Microbiol. Infect. Dis. **30**:309–327.
10. **Foung, S. K., B. Taidi, D. Ness, and F. C. Grumet.** 1986. A monoclonal antibody against HLA-A11 and A24. Hum. Immunol. **15**:316–319.
11. **Furutsuki, T., N. Hosoya, A. Kawana-Tachikawa, M. Tomizawa, T. Odawara, M. Goto, Y. Kitamura, T. Nakamura, A. D. Kelleher, D. A. Cooper, and A. Iwamoto.** 2004. Frequent transmission of cytotoxic-T-lymphocyte escape mutants of human immunodeficiency virus type 1 in the highly HLA-A24-positive Japanese population. J. Virol. **78**:8437–8445.
12. **Gao, W., A. Tamin, A. Soloff, L. D'Aiuto, E. Nwanegbo, P. D. Robbins, W. J. Bellini, S. Barratt-Boyes, and A. Gambotto.** 2003. Effects of a SARS-associated coronavirus vaccine in monkeys. Lancet **362**:1895–1896.
13. **Hatakeyama, S., Y. Matsuoka, H. Ueshiba, N. Komatsu, K. Itoh, S. Shichijo, T. Kanai, M. Fukushi, I. Ishida, T. Kirikae, T. Sasazuki, and T. Miyoshi-Akiyama.** 2008. Dissection and identification of regions required to form pseudoparticles by the interaction between the nucleocapsid (N) and membrane (M) proteins of SARS coronavirus. Virology **380**:99–108.
14. **He, Y., Y. Zhou, H. Wu, Z. Kou, S. Liu, and S. Jiang.** 2004. Mapping of antigenic sites on the nucleocapsid protein of the severe acute respiratory syndrome coronavirus. J. Clin. Microbiol. **42**:5309–5314.
15. **Kjer-Nielsen, L., C. S. Clements, A. W. Purcell, A. G. Brooks, J. C. Whisstock, S. R. Burrows, J. McCluskey, and J. Rossjohn.** 2003. A structural basis for the selection of dominant alphabeta T cell receptors in antiviral immunity. Immunity **18**:53–64.
16. **Kohyama, S., S. Ohno, T. Suda, M. Taneichi, S. Yokoyama, M. Mori, A. Kobayashi, H. Hayashi, T. Uchida, and M. Matsui.** 2009. Efficient induction of cytotoxic T lymphocytes specific for severe acute respiratory syndrome (SARS)-associated coronavirus by immunization with surface-linked liposomal peptides derived from a non-structural polyprotein 1a. Antiviral Res. **84**:168–177.
17. **Kuzushima, K., N. Hayashi, H. Kimura, and T. Tsurumi.** 2001. Efficient identification of HLA-A*2402-restricted cytomegalovirus-specific CD8(+) T-cell epitopes by a computer algorithm and an enzyme-linked immunospot assay. Blood **98**:1872–1881.
18. **Laskowski, R. A., M. W. Macarthur, D. S. Moss, and J. M. Thornton.** 1993. Procheck—a program to check the stereochemical quality of protein structures. J. Appl. Crystallogr. **26**:283–291.
19. **Lee, L. Y., D. L. A. Ha, C. Simmons, M. D. de Jong, N. V. Chau, R. Schumacher, Y. C. Peng, A. J. McMichael, J. J. Farrar, G. L. Smith, A. R. Townsend, B. A. Askonas, S. Rowland-Jones, and T. Dong.** 2008. Memory T cells established by seasonal human influenza A infection cross-react with avian influenza A (H5N1) in healthy individuals. J. Clin. Invest. **118**:3478–3490.
20. **Li, C. K., H. Wu, H. Yan, S. Ma, L. Wang, M. Zhang, X. Tang, N. J. Temperton, R. A. Weiss, J. M. Brenchley, D. C. Douek, J. Mongkolsapaya, B. H. Tran, C. L. Lin, G. R. Screaton, J. L. Hou, A. J. McMichael, and X. N. Xu.** 2008. T cell responses to whole SARS coronavirus in humans. J. Immunol. **181**:5490–5500.
21. **Li, T., J. Xie, Y. He, H. Fan, L. Baril, Z. Qiu, Y. Han, W. Xu, W. Zhang, H. You, Y. Zuo, Q. Fang, J. Yu, Z. Chen, and L. Zhang.** 2006. Long-term persistence of robust antibody and cytotoxic T cell responses in recovered patients infected with SARS coronavirus. PLoS One **1**:e24.
22. **Liu, J., Y. Sun, J. Qi, F. Chu, H. Wu, F. Gao, T. Li, J. Yan, and G. F. Gao.** 2010. The membrane protein of severe acute respiratory syndrome coronavirus acts as a dominant immunogen revealed by a clustering region of novel functional and structural defined cytotoxic T-lymphocyte epitopes. J. Infect. Dis. **202**:1171–1180.
23. **Liu, S. J., C. H. Leng, S. P. Lien, H. Y. Chi, C. Y. Huang, C. L. Lin, W. C. Lian, C. J. Chen, S. L. Hsieh, and P. Chong.** 2006. Immunological characterizations of the nucleocapsid protein based SARS vaccine candidates. Vaccine **24**:3100–3108.
24. **Ma, Y., Y. J. Feng, D. Liu, and G. F. Gao.** 2009. Avian influenza virus, Streptococcus suis serotype 2, severe acute respiratory syndrome-coronavirus and beyond: molecular epidemiology, ecology and the situation in China. Philos. Trans. R. Soc. Lond. B Biol. Sci. **364**:2725–2737.
25. **Maryanski, J. L., J. L. Casanova, K. Falk, H. Gournier, C. Jaulin, P. Kourilsky, F. A. Lemonnier, R. Luthy, H. G. Rammensee, O. Rotzschke, C. Servis, and J. A. Lopez.** 1997. The diversity of antigen-specific TCR repertoires reflects the relative complexity of epitopes recognized. Hum. Immunol. **54**:117–128.
26. **Masters, P. S.** 2006. The molecular biology of coronaviruses. Adv. Virus Res. **66**:193–292.
27. **Mathew, A., M. Terajima, K. West, S. Green, A. L. Rothman, F. A. Ennis, and J. S. Kennedy.** 2005. Identification of murine poxvirus-specific CD8(+) CTL epitopes with distinct functional profiles. J. Immunol. **174**:2212–2219.
28. **Meijers, R., C. C. Lai, Y. Yang, J. H. Liu, W. Zhong, J. H. Wang, and E. L. Reinherz.** 2005. Crystal structures of murine MHC class I H-2 D(b) and K(b) molecules in complex with CTL epitopes from influenza A virus: implications for TCR repertoire selection and immunodominance. J. Mol. Biol. **345**:1099–1110.
29. **Messaoudi, I., J. A. Guevara Patino, R. Dyall, J. LeMaoult, and J. Nikolich-Zugich.** 2002. Direct link between *mhc* polymorphism, T cell avidity, and diversity in immune defense. Science **298**:1797–1800.
30. **Middleton, D., L. Menchaca, H. Rood, and R. Komerofsky.** 2003. New allele frequency database: http://www.allelefrequencies.net. Tissue Antigens **61**:403–407.
31. **Ohno, S., S. Kohyama, M. Taneichi, O. Moriya, H. Hayashi, H. Oda, M. Mori, A. Kobayashi, T. Akatsuka, T. Uchida, and M. Matsui.** 2009. Synthetic peptides coupled to the surface of liposomes effectively induce SARS coronavirus-specific cytotoxic T lymphocytes and viral clearance in HLA-A*0201 transgenic mice. Vaccine **27**:3912–3920.
32. **Peng, H., L. T. Yang, L. Y. Wang, J. Li, J. Huang, Z. Q. Lu, R. A. Koup, R. T. Bailer, and C. Y. Wu.** 2006. Long-lived memory T lymphocyte responses against SARS coronavirus nucleocapsid protein in SARS-recovered patients. Virology **351**:466–475.
33. **Poon, L. L., Y. Guan, J. M. Nicholls, K. Y. Yuen, and J. S. Peiris.** 2004. The aetiology, origins, and diagnosis of severe acute respiratory syndrome. Lancet Infect. Dis. **4**:663–671.
34. **Price, D. A., S. M. West, M. R. Betts, L. E. Ruff, J. M. Brenchley, D. R. Ambrozak, Y. Edghill-Smith, M. J. Kuroda, D. Bogdan, K. Kunstman, N. L. Letvin, G. Franchini, S. M. Wolinsky, R. A. Koup, and D. C. Douek.** 2004. T cell receptor recognition motifs govern immune escape patterns in acute SIV infection. Immunity **21**:793–803.
35. **Rammensee, H., J. Bachmann, N. P. Emmerich, O. A. Bachor, and S. Stevanovic.** 1999. SYFPEITHI: database for MHC ligands and peptide motifs. Immunogenetics **50**:213–219.
36. **Rota, P. A., M. S. Oberste, S. S. Monroe, W. A. Nix, R. Campagnoli, J. P. Icenogle, S. Penaranda, B. Bankamp, K. Maher, M. H. Chen, S. Tong, A. Tamin, L. Lowe, M. Frace, J. L. DeRisi, Q. Chen, D. Wang, D. D. Erdman, T. C. Peret, C. Burns, T. G. Ksiazek, P. E. Rollin, A. Sanchez, S. Liffick, B. Holloway, J. Limor, K. McCaustland, M. Olsen-Rasmussen, R. Fouchier, S. Gunther, A. D. Osterhaus, C. Drosten, M. A. Pallansch, L. J. Anderson, and W. J. Bellini.** 2003. Characterization of a novel coronavirus associated with severe acute respiratory syndrome. Science **300**:1394–1399.
37. **Schlagenhauf, P., and H. Ashraf.** 2003. Severe acute respiratory syndrome spreads worldwide. Lancet **361**:1017.
38. **Slifka, M. K., and J. L. Whitton.** 2001. Functional avidity maturation of CD8(+) T cells without selection of higher affinity TCR. Nat. Immunol. **2**:711–717.
39. **Stewart-Jones, G. B., A. J. McMichael, J. I. Bell, D. I. Stuart, and E. Y. Jones.** 2003. A structural basis for immunodominant human T cell receptor recognition. Nat. Immunol. **4**:657–663.
40. **Sun, Y., J. Liu, M. Yang, F. Gao, J. Zhou, Y. Kitamura, B. Gao, P. Tien, Y. Shu, A. Iwamoto, Z. Chen, and G. F. Gao.** 2010. Identification and structural definition of H5-specific CTL epitopes restricted by HLA-A*0201 derived from the H5N1 subtype of influenza A viruses. J. Gen. Virol. **91**:919–930.
41. **Sylvester-Hvid, C., M. Nielsen, K. Lamberth, G. Roder, S. Justesen, C. Lundegaard, P. Worning, H. Thomadsen, O. Lund, S. Brunak, and S. Buus.** 2004. SARS CTL vaccine candidates; HLA supertype-, genome-wide scanning and biochemical validation. Tissue Antigens **63**:395–400.
42. **Tomiyama, H., K. Miwa, H. Shiga, Y. I. Moore, S. Oka, A. Iwamoto, Y. Kaneko, and M. Takiguchi.** 1997. Evidence of presentation of multiple HIV-1 cytotoxic T lymphocyte epitopes by HLA-B*3501 molecules that are associated with the accelerated progression of AIDS. J. Immunol. **158**:5026–5034.
43. **Tsao, Y. P., J. Y. Lin, J. T. Jan, C. H. Leng, C. C. Chu, Y. C. Yang, and S. L. Chen.** 2006. HLA-A*0201 T-cell epitopes in severe acute respiratory syndrome (SARS) coronavirus nucleocapsid and spike proteins. Biochem. Biophys. Res. Commun. **344**:63–71.
44. **Turner, S. J., K. Kedzierska, H. Komodromou, N. L. La Gruta, M. A. Dunstone, A. I. Webb, R. Webby, H. Walden, W. Xie, J. McCluskey, A. W. Purcell, J. Rossjohn, and P. C. Doherty.** 2005. Lack of prominent peptide-major histocompatibility complex features limits repertoire diversity in virus-specific CD8+ T cell populations. Nat. Immunol. **6**:382–389.
45. **Tynan, F. E., S. R. Burrows, A. M. Buckle, C. S. Clements, N. A. Borg, J. J. Miles, T. Beddoe, J. C. Whisstock, M. C. Wilce, S. L. Silins, J. M. Burrows, L. Kjer-Nielsen, L. Kostenko, A. W. Purcell, J. McCluskey, and J. Rossjohn.** 2005. T cell receptor recognition of a 'super-bulged' major histocompatibility complex class I-bound peptide. Nat. Immunol. **6**:1114–1122.
46. **Wang, B., H. Chen, X. Jiang, M. Zhang, T. Wan, N. Li, X. Zhou, Y. Wu, F. Yang, Y. Yu, X. Wang, R. Yang, and X. Cao.** 2004. Identification of an HLA-A*0201-restricted CD8+ T-cell epitope SSp-1 of SARS-CoV spike protein. Blood **104**:200–206.
47. **Wang, Y. D., W. Y. Sin, G. B. Xu, H. H. Yang, T. Y. Wong, X. W. Pang, X. Y. He, H. G. Zhang, J. N. Ng, C. S. Cheng, J. Yu, L. Meng, R. F. Yang, S. T. Lai, Z. H. Guo, Y. Xie, and W. F. Chen.** 2004. T-cell epitopes in severe acute respiratory syndrome (SARS) coronavirus spike protein elicit a specific T-cell immune response in patients who recover from SARS. J. Virol. **78**:5612–5618.
48. **Zakhartchouk, A. N., S. Viswanathan, J. B. Mahony, J. Gauldie, and L. A. Babiuk.** 2005. Severe acute respiratory syndrome coronavirus nucleocapsid protein expressed by an adenovirus vector is phosphorylated and immunogenic in mice. J. Gen. Virol. **86**:211–215.
49. **Zhou, M., D. Xu, X. Li, H. Li, M. Shan, J. Tang, M. Wang, F. S. Wang, X. Zhu, H. Tao, W. He, P. Tien, and G. F. Gao.** 2006. Screening and identification of severe acute respiratory syndrome-associated coronavirus-specific CTL epitopes. J. Immunol. **177**:2138–2145.

Biochemical and Biophysical Research Communications 393 (2010) 598–602

Contents lists available at ScienceDirect

Biochemical and Biophysical Research Communications

journal homepage: www.elsevier.com/locate/ybbrc

Influence of polymorphism in dendritic cell-specific intercellular adhesion molecule-3-grabbing nonintegrin-related (*DC-SIGNR*) gene on HIV-1 trans-infection

Dayong Zhu [a], Ai Kawana-Tachikawa [a], Aikichi Iwamoto [a,b,c], Yoshihiro Kitamura [a,b,c,*]

[a] *Division of Infectious Diseases, Advanced Clinical Research Center, Institute of Medical Science, University of Tokyo, 4-6-1 Shirokanedai, Minato-ku, Tokyo 108-8639, Japan*
[b] *Research Center for Asian Infectious Diseases, Institute of Medical Science, University of Tokyo, 4-6-1 Shirokanedai, Minato-ku, Tokyo 108-8639, Japan*
[c] *China-Japan Joint Laboratory of Molecular Immunology and Molecular Microbiology, Institute of Microbiology, Chinese Academy of Sciences, Olympic Park of Chinese Academy of Sciences, No. 1 Beichen West Road, Chaoyang District, Bejing 100101, China*

ARTICLE INFO

Article history:
Received 30 January 2010
Available online 10 February 2010

Keywords:
Dendritic cell-specific intercellular adhesion molecule-3-grabbing nonintegrin-related
Polymorphism
Trans-infection
Human immunodeficiency virus

ABSTRACT

The dendritic cell-specific intercellular adhesion molecule-3-grabbing nonintegrin (DC-SIGN) and DC-SIGN-related (DC-SIGNR) molecules on the cell surface are known to enhance human immunodeficiency virus type 1 (HIV-1) infection by capturing the virions and transmitting them to CD4+ T-cell, a process termed trans-infection. The neck region and carbohydrate recognition domain of the two proteins are important for efficient binding to the HIV-1 envelope protein. DC-SIGNR is polymorphic in Exons 4 and 5 that encode the neck region and carbohydrate recognition domain, respectively; the former contains a variable number of tandem repeats, and the latter the SNP (rs2277998). Since it remains unclear whether the DC-SIGNR polymorphism is related to the risk of HIV-1 infection, we tested possible effects of the polymorphism on HIV-1 trans-infection efficiency, by constructing six kinds of cDNAs encoding DC-SIGNR variants with various numbers of repeat units and various SNP. We were able to express the variants on the surface of Raji cells, a human B cell line. Flow cytometry showed that all the tested DC-SIGNR molecules were efficiently expressed on the cell surface at various levels; the assay for HIV trans-infection efficacy showed that all the tested variants had that activity with different efficacy levels. We found a correlation between the HIV trans-infection efficiency and the mean fluorescent intensity of DC-SIGNR expression ($R^2 = 0.95$). Thus, our results suggest that the variation of the tested DC-SIGNR genotypes affects the efficacy of trans-infection by affecting the amounts of the protein expressed on the cell surface.

Introduction

The dendritic cell-specific intercellular adhesion molecule-3-grabbing nonintegrin (DC-SIGN; also known as C-type lectin domain family 4, member L (CLEC4L) or CD209) is a type II membrane protein expressed mainly on dendritic cells (DCs) and has been found to capture human immunodeficiency virus type 1 (HIV-1) by binding to HIV-1 Env and transmit it to $CD4^+$ cells; this process is called trans-infection [1,2]. DC-SIGNR (DC-SIGN-related; also known as DC-SIGN2, CD299, CD209L, L-SIGN, or C-type lectin domain family 4, member M (CLEC4M)) mainly expressed in the lymph nodes and liver is a homologue of DC-SIGN and are thought to affect HIV-1 infection by the same process [3–5]. DC-SIGNR consists of a short intracytoplasmatic region; a neck region, which contains tandem repeats of a highly conserved 23-amino acid sequence; and a carbohydrate recognition domain (CRD) [6,7]. Exon 4 encodes the neck domain and Exons 5–7 encode CRD (Fig. 1A) [7–9]. The neck region and CRD are supposed to play an important role in binding to viral glycoproteins such as HIV-1 Env [6,10–15]. The neck region is essential for lectin tetramerization, which is believed to be important for binding to pathogens [11,14–16]. The CRD of DC-SIGNR recognizes glycans on viral envelope glycoprotein and is essential for pathogen binding [6,12,17].

The *DC-SIGN* gene polymorphism is rare, while *DC-SIGNR* gene polymorphism is found frequently in different ethnic groups [3,8,9,18–21]. There is a *DC-SIGNR* gene polymorphism in Exon 4 that differs in number of repeats, which varies from 3 to 10 [3,8,9,11,18,19,21]. Individuals can be heterozygous or homozygous for these *DC-SIGNR* alleles. The *DC-SIGNR* allele with seven repeat units is the most common among different ethnic groups and is considered wild type [3,18]. *DC-SIGNR* alleles with five, seven,

* Corresponding author. Address: Research Center for Asian Infectious Diseases, Institute of Medical Science, University of Tokyo, 4-6-1 Shirokanedai, Minato-ku, Tokyo 108-8639, Japan. Fax: +81 354495496.
E-mail addresses: zhu@ims.u-tokyo.ac.jp (D. Zhu), aikawana@ims.u-tokyo.ac.jp (A. Kawana-Tachikawa), aikichi@ims.u-tokyo.ac.jp (A. Iwamoto), yochan@ims.u-tokyo.ac.jp, kitamura@im.ac.cn (Y. Kitamura).

0006-291X/$ - see front matter © 2010 Elsevier Inc. All rights reserved.
doi:10.1016/j.bbrc.2010.02.021

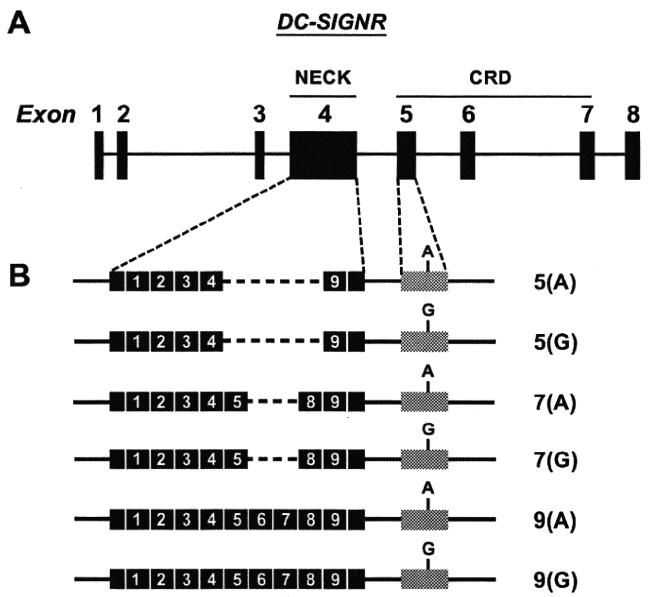

Fig. 1. *DC-SIGNR* gene and cDNAs. (A) *DC-SIGNR* gene organization. The horizontal line represents the *DC-SIGNR* gene on human Chromosome 19. The closed boxes represent exons. Exon 4 encodes the neck domain and Exons 5–7 encode the carbohydrate recognition domains (CDRs). (B) Structures of the six kinds of *DC-SIGNR* cDNA used for the study. The thin horizontal line represents the *DC-SIGNR* full-length cDNA. The numbered closed boxes at the left represent Exon 4 containing 5, 7, or 9 repeat units. The shaded boxes at right represent Exon 5, on which the SNP (GenBank Accession No. rs2277998) genotypes are shown.

and nine repeat units are frequently found in both Asians and Caucasians [3,8,9,18,19]. One SNP (rs2277998, IMS-JST025121) in Exon 5 has been confirmed in CDR of *DC-SIGNR* in Asians [8,9]. The A to G change at this SNP position results in Asp substitution for Asn.

A potential association of the *DC-SIGNR* polymorphism and risk of HIV-1 infection is currently under debate. The association of *DC-SIGNR* polymorphism and HIV-1 susceptibility has been shown in some studies [8,19,22], whereas no significant association has been shown in other studies either in vivo or in vitro [18,23,24]. Among the positive studies, no common conclusion has been reached presumably due to the size of the target population and ethnicity. Moreover, it is noteworthy that differential HIV-1 susceptibility of males and females among the spouses of HIV-seropositive individuals in Thais has been recently reported: heterozygous 7/5 and 9/5 repeat along with the A allele at the rs2277998 position of *DC-SIGNR* showed a reduced risk in HIV-1 infection in the HIV-1-exposed seronegative females [8]. To help understand molecular basis of the above-mentioned association, we have hypothesized that the molecules encoded by those various alleles exhibit different efficacy in trans-infection of HIV-1. In this study, we have constructed *DC-SIGNR* complementary DNAs of all the possible combinations of polymorphic genotypes in Exons 4 and 5, and have assayed the efficacy of HIV-1 trans-infection by the molecules encoded by these cDNAs in vitro.

Materials and methods

Plasmid construction. The plasmid pcDNA3-DC-SIGNR(7G), which contains full-length *DC-SIGNR* cDNA with seven repeat units in Exon 4 and G at the SNP (rs2277998) in Exon 5, was obtained from the NIH AIDS Research and Reference Program (Suite 200, Germantown, MD 20874, USA) [4]. To construct *DC-SIGNR* mutant with A at the SNP in Exon 5, we amplified a partial Exon 5 region of containing A at the SNP by PCR using genomic DNA of an individual, whose genotype had been confirmed. Then we cut out the BbvCI–PflMI fragment from the PCR product, and inserted it into the corresponding domain of pcDNA3-DC-SIGNR (7G). The resulting plasmid is termed pcDNA3-DC-SIGNR (7A). To construct *DC-SIGNR* mutants with five or nine repeat units in Exon 4, we used genomic DNA of individuals whose genotype had been confirmed. In brief, we amplified a partial Exon 4 region containing five or nine repeat units by PCR. Then we cut out the XagI–BbsI fragments containing the repeats, inserted each of them into the corresponding site of pcDNA3-DC-SIGNR (7G) or pcDNA3-DC-SIGNR (7A). The resulting plasmids with five or nine repeat units are pcDNA3-DC-SIGNR (5G) and pcDNA3-DC-SIGNR (5A), or pcDNA3-DC-SIGNR (9G) and pcDNA3-DC-SIGNR (9A), respectively (Fig. 1B). The DNA sequence of their *DC-SIGNR*-coding regions was confirmed by DNA sequencing. We obtained and used human genomic DNA under written informed consents. This study has been certified by a Bioethic Committee and Biosafety Committee, Institute of Medical Science, University of Tokyo (the approved ID 11-2-0329).

Cells. 293T cells (a human embryonic kidney cell line) were propagated in Dulbecco's modified Eagle's medium (DMEM) (Sigma, St. Louis, MO, USA) supplemented with 10% fetal bovine serum, penicillin (Sigma), and streptomycin (Sigma). Raji, Raji/DC-SIGN [25] and MT4 cells [26] (NIH AIDS Research and Reference Reagent Program, MD, USA, Raji cells cat. no. 9944, Raji/DC-SIGN cells cat. no. 9945, MT4 cells cat. no. 25 070567) were maintained in RPMI 1640 (Sigma) containing 10% fetal bovine serum, penicillin, and streptomycin. MT4 cells are highly susceptible to HIV-1 infection and are used as target cells in HIV-l trans-infection experiments. All cells were grown at 37 °C in 5% CO_2.

Antibodies. Phycoerythrin-conjugated mouse anti-human monoclonal antibodies (mAbs) against DC-SIGNR (Clones 120604, R&D Systems, Minneapolis, MN) and DC-SIGN (clone 120507, R&D Systems, Minneapolis, MN) were used. APC-labeled anti-CD4 mAb (Catalog No. 341095; BD Biosciences, San Jose, CA) was used in trans-infection experiments. FACS analysis was performed with a FACSCalibur flow cytometer (BD, San Jose, CA).

Generation of stable and high DC-SIGNR expression cells. Raji cells were transfected with one of the six plasmids by electroporation with a Gene Pulser XCell System (Bio-Rad, Hercules, CA). Briefly, 2×10^6 exponentially growing cells were suspended in a total volume of 200 μl of PBS containing 10 μg of each plasmid DNA. Cells were electroporated at 190 V and 1000 μF, were suspended in 2 ml of the growth medium, seeded in 6-well plates, and were maintained at 37 °C. Forty-eight hours after transfection, a half of the cells were analyzed for DC-SIGNR expression by flow cytometry. To obtain stable DC-SIGNR-expressing cells (Raji/DC-SIGNR), we continued culturing the remaining half of the transfected Raji cells with 1.2 mg/ml G418 (Sigma) to collect G418-resistant cells. We confirmed stable DC-SIGNR expression with a FACSCalibur. To obtain cells with high levels of DC-SIGNR expression, these $G418^R$ Raji cells were sorted with a FACSAria (BD) sorter. After culturing these cells with G418 for 6 days, we verified the DC-SIGNR expression and subjected the cells to trans-infection assay. A CRD-specific mAb 120604 was used for sorting and analysis of DC-SIGNR expression. Since the main modification was introduced in the neck domain (Exon 4) and only one amino acid change was introduced in Exon 5, the six constructs we tested can be detected equally by mAb 120604.

Production of HIV-1 expressing GFP. We produced $HIV\text{-}1_{NL\text{-}EGFP}$ stock virus by transfecting 293T cells with the plasmid pNL-EGFP [27] using a lipofectamine 2000 (Invitrogen) as recommended by the manufacturer. We replaced the culture medium with the fresh medium 24 h after transfection and harvested the medium 48 h after transfection. The harvested medium was stored at −80 °C until use. To determine virus titers, we infected 2×10^5 MT4 cells with 500 μl virus sample for 2 h in 37 °C, added 2 ml of the

complete medium, cultured them for additional 24 h, and determined the ratio of EGFP-positive cells in the total cells by flow cytometry. At the same time, ELISA assays for capsid protein (p24) were performed to determine the amount of p24 (ZeptoMetrix Corporation, New York, USA).

Assay for DC-SIGNR-mediated HIV-1 trans-infection. HIV-1 capture and transmission by the cells with different DC-SIGNR alleles were assessed in a co-cultivation assay. The six kinds of sorted Raji/DC-SIGNR, Raji/DC-SIGN and Raji cells were used as donor cells. The donor cells (2.5×10^5) were incubated with 400 μl of HIV-$1_{NL\text{-}EGFP}$ (p24 = 145 ng) in a 15 ml-tube for 3 h at 37 °C to allow the virions to bind to Raji cells expressing DC-SIGNR. Then, the cells were washed with 1 ml of phosphate-buffered saline (PBS) and co-cultured with MT4 target cells (1×10^5) in 1 ml of the culture medium in 24-well plates. Co-culturing them for 24 h, we stained them with an anti-CD4 antibody and analyzed for GFP and CD4 expression by flow cytometry. HIV-1 trans-infection efficiency was expressed by the percentage of EGFP-positive cells among the CD4-positive cells.

Results

Various types of genetic polymorphism have been described in *DC-SIGNR*. They include the variable numbers of tandem repeat of a 69 bp sequence unit in Exon 4 and an SNP (rs2277998 also known as IMS-JST025121) in Exon 5 [3,8,9,11]. The *DC-SIGNR* alleles with five, seven, and nine repeat units in Exon 4 are frequently found in both Asians and Caucasians [3,8,9,18]. The *DC-SIGNR* allele with A or G at the SNP in Exon 5 is frequently found in Asians [8,9]. Although these types of polymorphism on Exons 4 and 5 are thought to affect the HIV-1 susceptibility [8,19], it is unclear whether the alleles exhibit different efficacy in promoting trans-infection of HIV-1. To clarify this question, we constructed six kinds of cDNA with all the possible combination of five, seven, or nine repeat units in Exon 4 along with A or G at the SNP in Exon 5 (Fig. 1B). Then we determined the efficiency of trans-infection by these *DC-SIGNR* alleles. Except the repeat number in the neck region and the nucleotide at the SNP, all the *DC-SIGNR* cDNAs used in this study exhibited the identical nucleotide sequences.

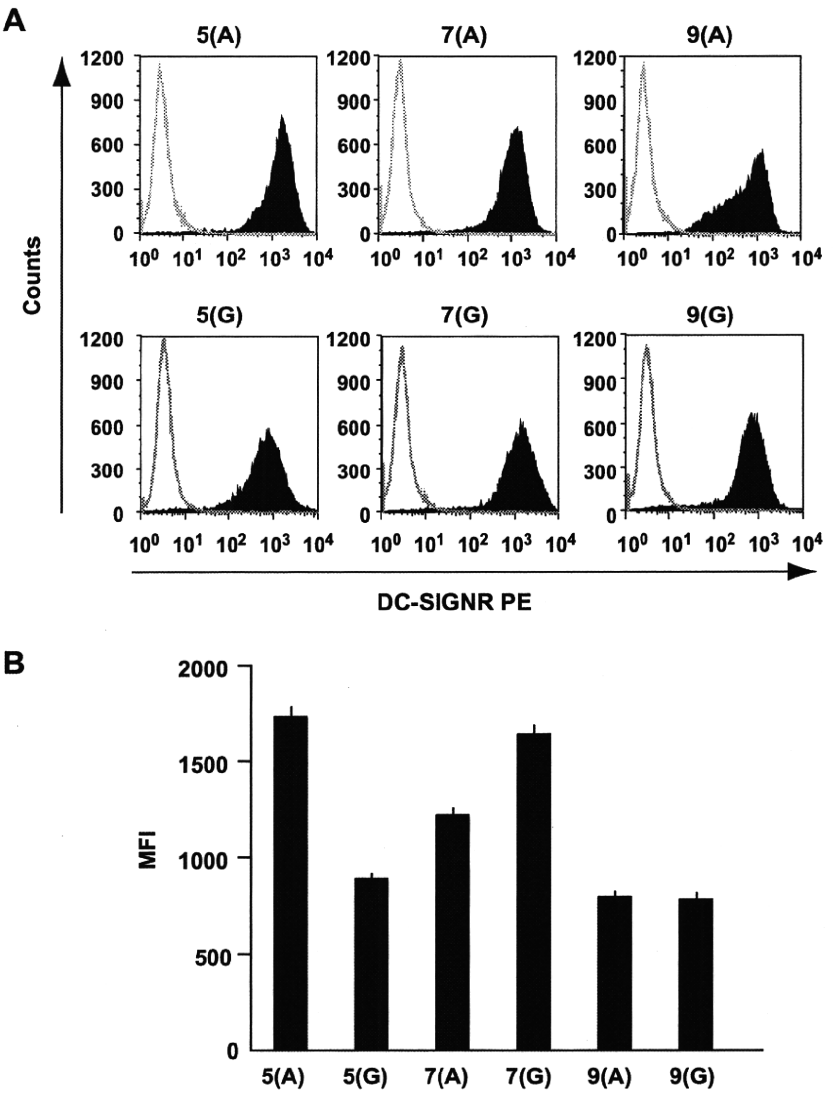

Fig. 2. The DC-SIGNR expression levels of Raji cells transfected with various DC-SIGNR cDNAs. (A) DC-SIGNR expression levels of DC-SIGNR^{high} Raji cells collected with FACS Aria are shown. On all histogram, the black-filled histograms represent staining with DC-SIGNR mAb staining, whereas the gray curves represent isotype control antibody. The control untransfected Raji cells showed a background level of antibody-binding (data not shown). (B) The bars represent the MFI of DC-SIGNR expression as determined by flow cytometry in three independent experiments.